Workshop on Forward Calorimetry at Future Linear Collider

13-15 September 2011
Vinča Institute of Nuclear Sciences
Belgrade, Serbia

Editor
Ivanka Božović – Jelisavčić

Published by:
Vinča Institute of Nuclear Sciences,
P. O. Box 522 11001 Belgrade, Serbia

For the Publisher: Jovan Nedeljković

Editors: Ivanka Božović - Jelisavčić, INN Vinča, Serbia

ISBN: 978-86-7306-114-6

Preface

Vinča Institute of Nuclear Sciences from Belgrade, Serbia is proud to host for the second time the Workshop of the Collaboration on Forward Calorimetry (FCAL) at future linear collider. Already the fact that this is the nineteenth meeting in the series of traditional workshops illustrates the continuous effort of the international community not only to instrument the forward region of the future linear collider to meet the requirements from physics, but also to improve the understanding of physics and machine related processes ongoing at the very low polar angles.

From an editor's point of view this Workshop was particularly interesting for bringing up an abundance of the test-beam results on performance of sensors for the forward region calorimeters tested for the first time as an integrated structure with the front-end electronics. In the scope of simulation studies a novel perspective on beam-related effects in the integral luminosity measurement at future linear collider was presented. Overall fifteen contributions are given in the course of the Workshop.

This meeting was supported by the Ministry of Education and Science of the Republic of Serbia as well as through the project OI171012 being realized at the Vinca Institute of Nuclear Sciences.

On behalf of the Organizing Committee,

Ivanka Božović – Jelisavčić

List of Committee Members

International Advisory Committee

Wolfgang Lohmann, DESY, Germany
Aharon Levy, Tel Aviv University, Israel
Lucie Linssen, CERN, Switzerland
Marek Idzik, AGH UST, Poland
Ivanka Božović - Jelisavčić, INN Vinča, Serbia

Local Organizing Committee:

Ivanka Božović - Jelisavčić, INN Vinča, Serbia
Ivan Smiljanić, INN Vinča, Serbia
Mila Pandurović, INN Vinča, Serbia
Tatjana Jovin, INN Vinča, Serbia
Predrag Ćirković, INN Vinča, Serbia
Stevan Jokić, INN Vinča, Serbia
Snežana Milosavljević (secretary), INN Vinča, Serbia

Table of Contents

Introduction

INTRODUCTION TO THE FCAL WORKSHOP

By

Wolfgang LOHMANN

DESY, Zeuthen, and Brandenburg University of Technology

This workshop happens in a time of challenging developments in particle physics. The LHC collider is delivering data of excellent quality and sensitivity giving us the optimism that groundbreaking discoveries will happen soon. Two technologies of a linear electron-positron colliders, the ILC and CLIC, are developed to be prepared for different energy range to investigate in detail new phenomena discovered by LHC. FCAL is part of the world wide R&D effort to develop the detector technologies for special calorimeters in the very forward region matching the challenge from Physics.

Key words: Linear collider detector R&D

INTRODUCTION

The LHC collider is is operated with excellent performance and will deliver data up to the end of the year with a sensitivity of several inverse femtobarn. These data will extend the range for the search of new phenomena considerably, and will lead within the electroweak standard theory to either a tighter mass limits for the Higgs boson or to an indication of a signal. Based on these results a guidance on future developments may become more clear.

To explore new phenomena discovered at the LHC a linear electron-positron collider will be the appropriate machine. Two concepts are pursued in world-wide collaborations. For the ILC, based on superconducting cavities, after more than a decade of successful R&D, the Engineering Design Report is worked out and will be released in 2012. CLIC, using normal conducting cavities but a new technology to obtain the accelerating power, made and important step forward by the release of a Conceptual Design Report just now.

For both facilities detector R&D is performed within world-wide collaborations. For two concepts of an ILD detector, ILD and SiD, Engineering Design Reports are under work and will be released together with the EDR of ILC. Two designs for CLIC detectors have been worked out and published recently together with the CLIC detectors.

FCAL is a R&D collaboration to develop the technologies for the instrumentation of the very ard region both at the ILC and CLIC.

THE FCAL COLLABORATION – RESULTS IN 2011

FCAL is a collaboration of 17 laboratories and university groups from around the world. The common goal is to work out a design of the forward region of detectors at a future linear electron-positron collider, to develop technologies for the detectors, and test prototypes of major components to perform a proof of principle. As

an example in Figure 1 is shown the very forward region of the CLIC detector. Two calorimeters are positioned there- the LumiCal to measure precisely the luminosity at larger polar angles and the BeamCal to improve the detector hermeticity and assist beam tuning.

This design is the results of detailed Monte Carlo simulation to optimize the design to ensure a precision of the luminosity measurement of better than 10^{-2} and minimize low energy backscattered particles.

Another important result was the simulation of the response of LumiCal for Bhabha scattering events at 1.5 TeV. As a result shower and background deposition profiles as shown in Figure 2 are obtained. These and more results are reported in the CLIC conceptional design report written in 2010 and 2011 and released in August 2011[1].

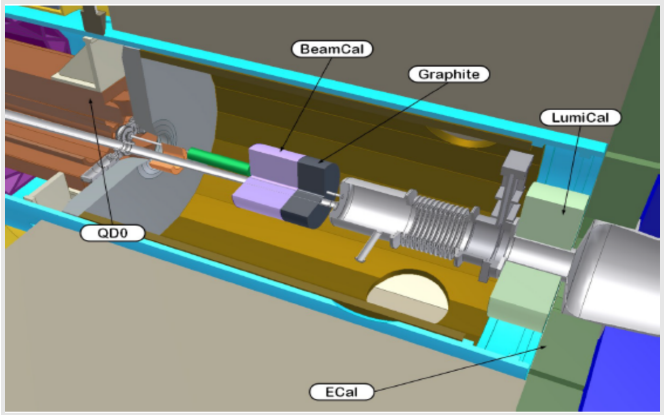

Figure 1 The very forward region of a detector at CLIC. LumiCal is positioned just behind the electromagnetic calorimeter and BeamCal in front of the beam focussing magnet.

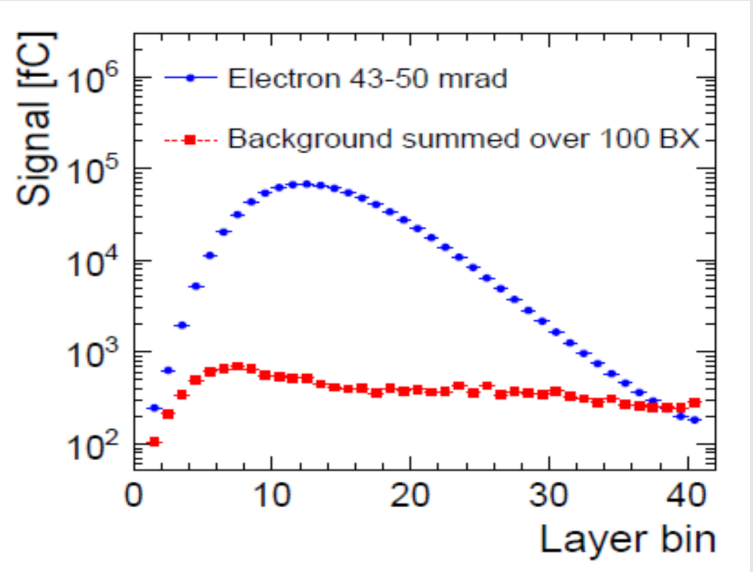

Figure 2 The energy profile of a shower of an Electron from Bhabha scattering and of background depositions as a function of the depth in LumiCal

In 2010 and 2011 two test-beam campaign have been finished successfully. For the first time sensor prototypes for both BeamCal and LumiCal have been connected with readout ASICs. The fully assembled sensors were positioned within several planes of a beam telescope and a few millions of triggers have been recorded. As an example, the distribution of hits on a pad sensor for BeamCal is shown in Figure 3.

More data will be taken in December 2011. Data analysis is one of the major topics ongoing in the collaboration and the results on the performance of several sensor planes for LumiCal and BeamCal will be the contribution of FCAL to the ILC detector Engineering design report.

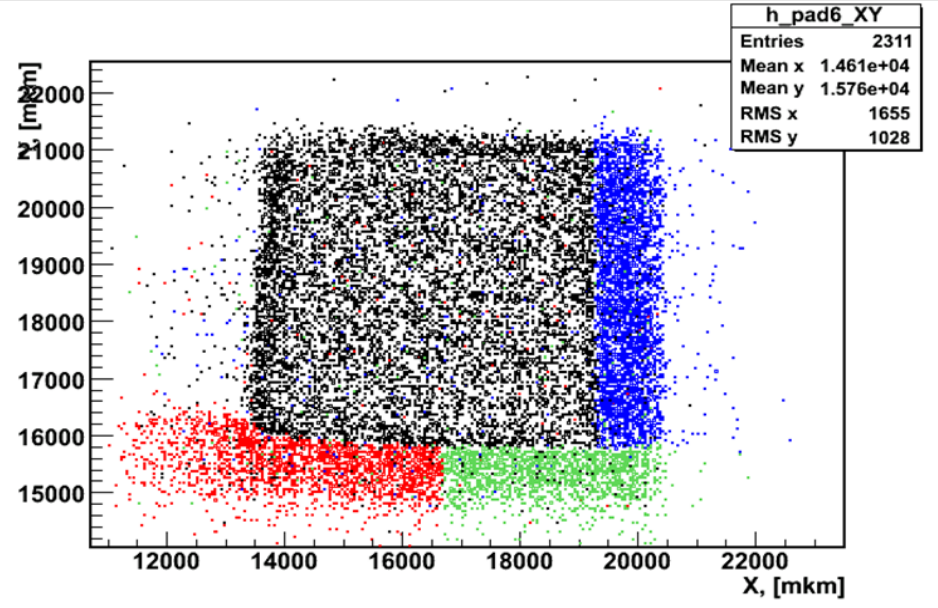

Figure 3 The distribution of hits on a fully instrumented sensor of BeamCal.

FCAL members have contributed to several conferences in 2011, e.g. to the EPS conference in Grenoble. Results on the performance of the pair monitor, a pixel detector just in front of BeamCal, have been recently published in NIM.

DATES AHEAD

End of September will be a Linear Collider Workshop in Granada, and for sure we should report there about our recent research results. In October we are invited to report about the progress of FCAL to the PRC of the DESY lab. This workshop will be devoted to prepare both reports.

REFERENCES

[1] CLIC Conceptual design report, Vol. 2, Physics and Detectors at CLIC, http://lcd.web.cern.ch/LCD/CDR/CDR.html88

Hardware and test beam results

STUDIES ON INNER DETECTORS ALIGNMENT IN ILD

By

J.A. AGUILAR[a,b], W. DANILUK[a], E. KIELAR[a], J. KOTUŁA[a], A. MOSZCZYŃSKI[a], K. OLIWA[a], B. PAWLIK[a], W. WIERBA[a] and L. ZAWIEJSKI[a]

[a]*Institute of Nuclear Physics PAN , Cracow, Poland*

[b]*AGH University of Science and Technology ,Poland*

Status of the alignment system for luminosity and vertex subdetectors of the ILD main detector is presented. The system will contain transparent position sensors, atunable laser and beam splitters in order to use frequency scanning interferometry to supply the required accuracy in displacement measurements. At first step the prototype of the system will be built for the luminosity detector and tested at an accelerator beam in combination with a high-granularity calorimeter module being developed within the AIDA project. Afterwards the system will be extended to the vertex detectors as well.

Key words: alignment, laser, transparent sensors, accuracy in luminosity measurements

1. INTRODUCTION

The International Large Detector (ILD) was prosed [1] as one the two main detectors for future exeriments at International Linear Collider [2]. The physics program at ILC requires high-precision measurements performed by all subdetectors of the ILD. This also concerns the inner subdetectors close to the interaction point: vertex (VTX,SIT,SET,FTD) and luminosity detector (LumiCal-L,LumiCal-R). Alignment of the whole subdetectors and their parts must be considered as an important element under the construction phase and later during their operation.

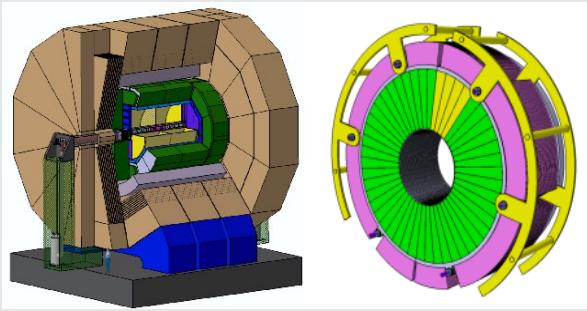

Figure 1. Top left: ILD detector; Bottom: Inner subdetectors: luminosity and vertex detectors together with the support tube (in grey). In addition one of the Lumical calorimeter is shown (top right).

The close neighboring of vertex detectors and LumiCal calorimeters (L and R) (see Fig. 1) suggests a common laser alignment system (LAS) may be considered for those subdetectors. The system is designed to measure the positions of these subdetectors and their components with several micrometers precision. The important for this will be knowledge of the QD0

magnet and beam pipe current positions. At first the prototype of LAS for LumiCal alone will be build and tested with a calorimeter module, which itself will be built under the tasks of the working package WP9.5 in AIDA [3], and then extended for vertex subdetectors.

2. LUMICAL ALIGNMENT

The proposed LAS will be based on Frequency Scanning Interferometry and transparent position sensors. The schematic view of the system is shown in Figure 2.

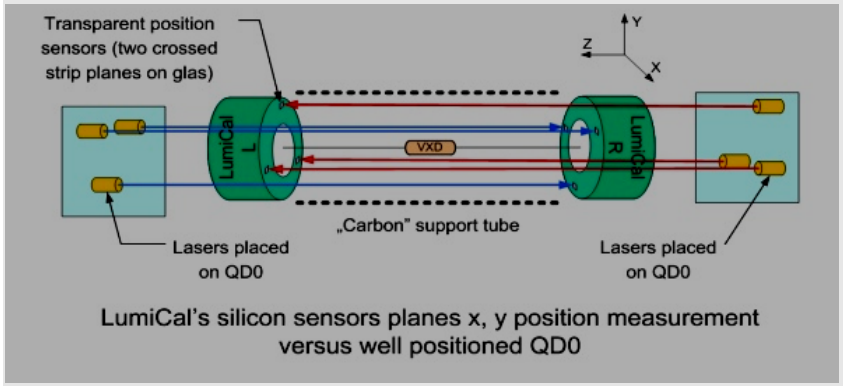

Figure 2. Laser beams from tunable laser in Frequency Scanning Interferometry method enable absolute distance measurements between two LumiCal calorimeters (L and R).

The position measurements of both (L/R) calorimeters will be performed in respect to the reference frames of the QD0 magnet or beam pipe. This is important as their current positions will be measured with very high accuracy. The laser beams proposed for absolute distance measurement between L and R calorimeters may go through additional carbon pipes glued to a carbon support tube. These laser beams together with transparent position sensors can be used in position measurements the individual elements of vertex detector (see Fig. 3).

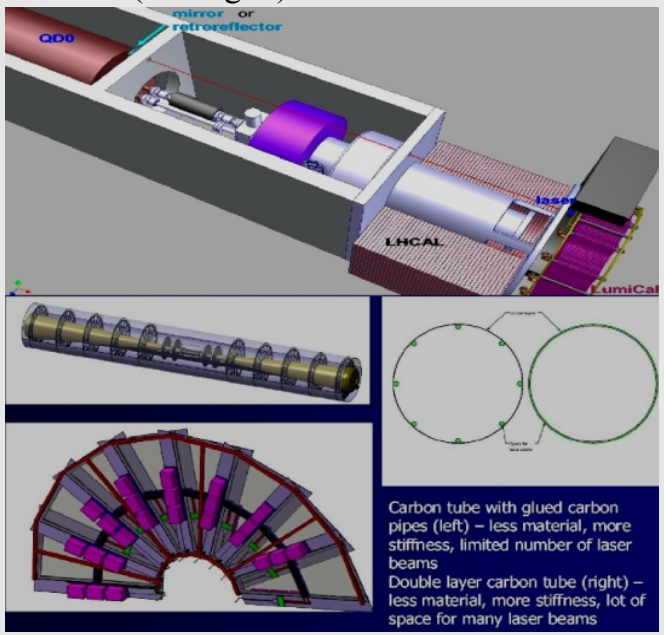

Figure 3. Top: The QD0 magnet as reference frame for LumiCal alignment. Bottom: The possible localization of the additional carbon pipes for laser beams from tunable laser. The transparent sensors can be placed on the disks of vertex detectors.

3. FSI

Frequency Scanning Interferometry (FSI) is robust and versatile technique where measurement of interferometer optical path differences is made using a tunable laser (different frequences). It provides an absolute distance measurement. The

tunable laser illuminates both the interferometer to be measured and a reference interferometer (pattern of distance). When the optical frequency is scanned a phase shift is induced in interferometers at rate which is proportional to the length of each interferometer. The phase shift in interferometers are compared to determine the ratio of interferometer lengths to high precision. The method has found application previously in the ATLAS experiment [4].

4. TRANSPARENT SENSORS

In ILD detector concept the transparent position sensors as element of LAS are considered for silicon the tracking system [1]. Wide studies under the EUDET project [5] give results on transparent sensors which can be used for this purpose. Figure 4 shows as example an infra-red laser beam traversing several transparent sensors with light absorption changing from 30 % to about 60 %. This transparent sensor property can be used in design of a multi-point laser-based alignment system where laser beam is split into several beams distributed along single optical fibres (colimators) traversing transparent sensors which measure the X and Y positions of targeted detectors.

In prototype of LAS for LumiCal the ZEUS MVD transparent sensors [6] will be used.

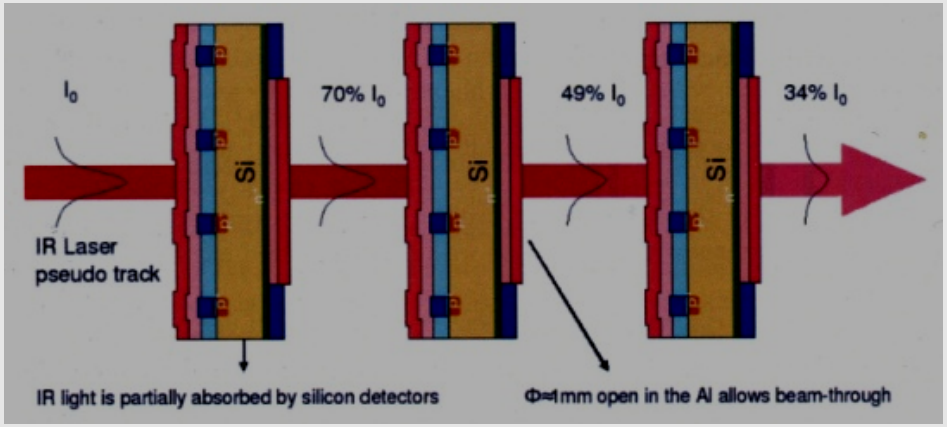

Figure 4. Scematic view of infra-red laser beam traversing several transparent sensors.

ZEUS MVD transparent sensors

The sensors were developed by Kroha et al. [7] and manufactured by EG&G Haimann Optoelectronics in Wiesbaden. They are identified as DPSD-516 sensors. Figure 5 descibes the structure of the sensors where a fully active, photo-sensitive layer is made as amorphous, hydrogenated silicon. The Indium Tin Oxide transparent upper and bottom electrodes are segmented in X and Y strip rows supplying high precision position measurements in these two coordinates with accuracy ~ 10 micrometers.

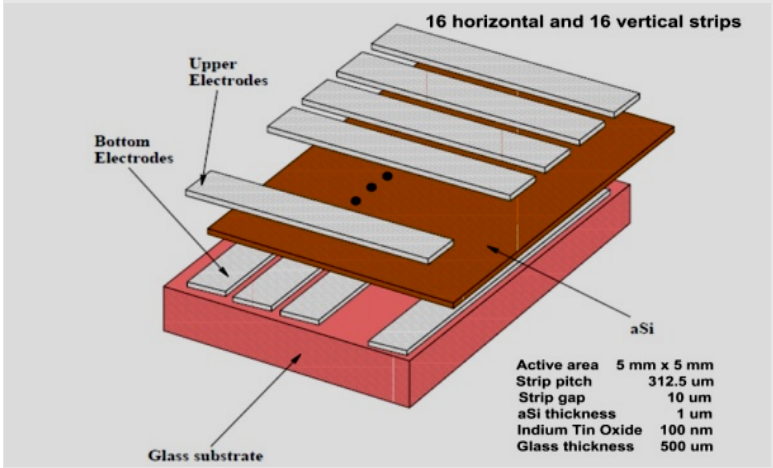

Figure 5. The DPSD-515 amorphous silicon strip sensor with 16 horizontal and vertical strips.

Figure 6 shows the general view of the sensor and its bonding to the flat readout cable. The same figure illustrate the sensor transparency to the infra- red light.

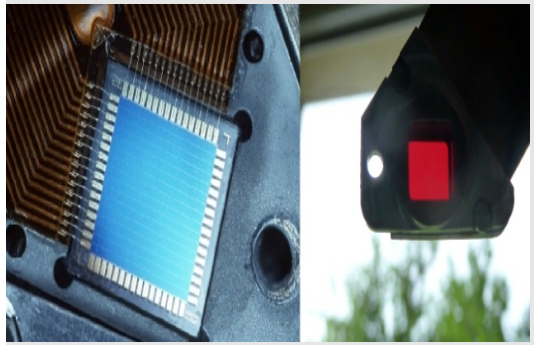

Figure 6. DPSD-516: Left: Sensor bonding to flat, readout cables: Right: A transparency to infra-red laser light.

The base property of DPSD-516 sensor is the value of its transmission of illuminated laser light with different wavelength . This is shown in Fig. 7.

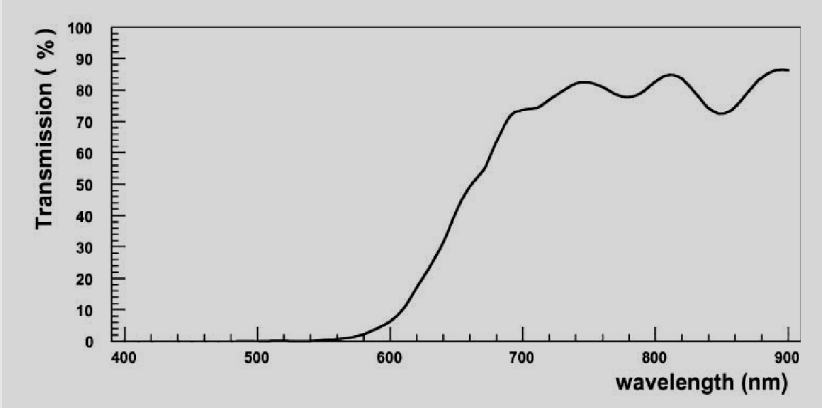

Figure 7. DPSD-516: The transmission as a function of wavelength.

Above wavelength 700 nm the plateau is visible with transmission above 85%. The consequence this is that high sensor transparency required a choice of the laser light with suitable wavelength ~ 780 nm. With high transmission rate one can used several sensors in one laser beam.

The schematic view of readout electronics is shown in Fig. 8

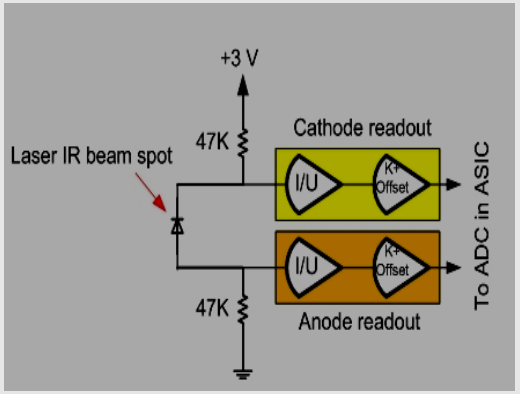

Figure 8. The scheme view of readout electronics

5. AIDA ACTIVITIES AND FUTURE PLANS

Inside the AIDA project [3] work on a prototype of LAS for LumiCal is going on. In the first step the DPSD sensors with an infra-red laser light illuminated sensors, will be mounted in laboratory to determine the parameters of the system. In the next step the system will be tested together with AIDA LumiCal prototype at DESY and CERN test beams. A schematic view for a simplified setup is shown in Fig. 9. A similar approach will be applied to build the prototype of FSI system. First a prototype will be mounted for laboratory test. Besides the tunable laser, interferometers, beam-splitters, optical fibres also other optical elements like retroreflectors, mirrors will be used. The simplified version of the proposed setup is shown in Fig.10. Goal in AIDA activity is to finally test the complete LAS system where transparent sensors and FSI will supply position measurements. The data aquisition system of LumiCal LAS will be included in global DAQ scheme which is being prepared within the AIDA project.

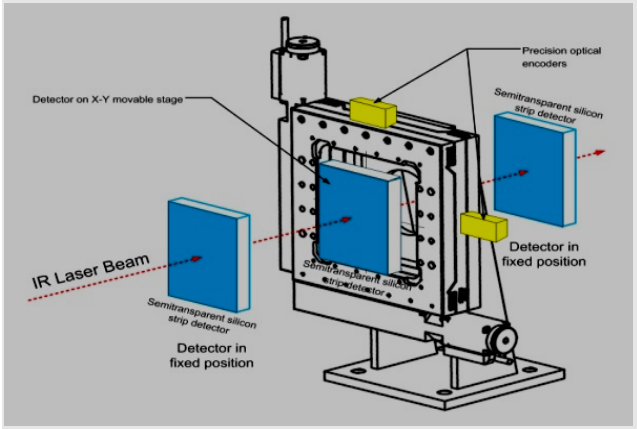

Figure 9. Proposed experimental set-up with transparent DPSD sensors for laboratory and test beam measurements

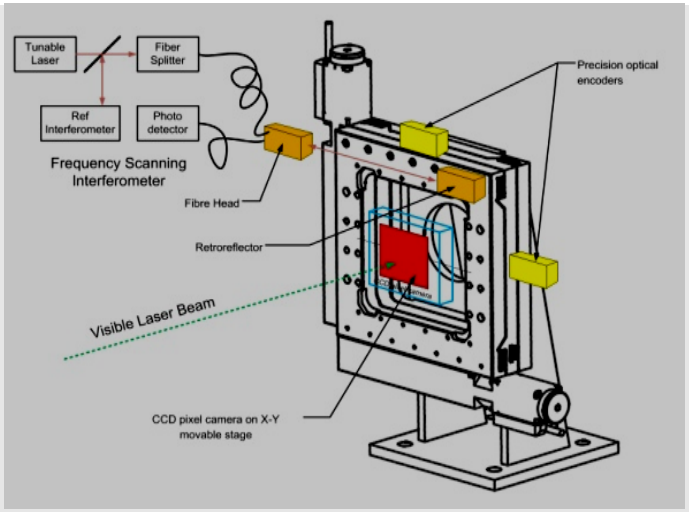

Figure 10. Proposed setup with FSI for laboratory and test beam measurements.

6. CONCLUSION

The laser alignment system for LumiCal and other inner ILD subdetectors is in the first stage of work. The important part of work will be connected with Monte Carlo simulations on design of the system and its optimalisation. The final shape of design requires collaboration between all inner subdetector groups participating in the ILD project. The final sytem for position measurement and monitoring will contain transparent sensor and FSI. It will be possible in future to replace the DPSD-516 sensors with the new generation like “AMY” sensors [8] connected with CMS experiment at LHC in CERN. Very important to the LAS is the selection of a very stable reference frame whose position during the data taking will be know with very high precision. One the best candidate is QD0 magnet. Other possibility is to choose beam pipe as such reference frame.

ACKNOWLEDGEMENTS

This work was partially supported by the European Commission within Framework Programme 7 Capacities, Grant Agreement number 262025.

REFERENCES

[1] The International Large Detector, Letter of Intent, DESY 2009-87; FERMILAB-PUB-09-682-E; KEK Report 2009-6.

[2] International Linear Collider, http://www.linearcollider.org/.

[3] AIDA (Advanced European Infrastructures for Detectors at Accelerators), http://aida.web.cern.ch/aida/index.html

[4] A. F. Fox-Murphy et al., Nucl. Instr. and Meth. A 383 (1996) 229; P. A. Coe et al., Meas. Sci. Technol. 15 (2004) 2175.

[5] M. Fernandez et al., “Semitransparent microstrip detectors for infrared laser alignment of particle trckers”, EUDET-Memo-2010-20, http://www.eudet.org/

[6] T. Matsushita et al., Nucl. Instr. and Meth. A 466 (2001) 383; K. Korcsak-Gorzo et al., Nucl. Inst. and Meth. A 580 (2007) 1227.

[7] W. Brum, H. Kroha and P. Widmann, Nucl. Instr. and Meth. A 367 (1995) 413.

[8] M. Fernandez et al., “Final production of novel IR-transparent microstrip silicon sensors ”, EUDET-Memo-2009-23 , http://www.eudet.org.

TEST BEAM PREPARATION OF GaAs SENSOR AND NEW R/O ELECTRONICS

By

O.NOVGORODOVA[1,2], H.HENSCHEL[1], W.LANGE[1], W.LOHMANN[1,2], S.SCHUWALOW[3]

(1) DESY, Zeuthen, Germany

(2) BTU Cottbus, Cottbus, Germany

(3) Hamburg University, Hamburg, Germany

Forward region of the future linear e+e- colliders is going to be instrumented with special calorimeters. Beam calorimeter (BeamCal) will be highly segmented, compact, radiation hard, cylindrical sandwich calorimeter. BeamCal prototype instrumented with GaAs sensor, ASIC's and specially designed for ILC ADC will be tested in DESY II test beam. Preparation for the next test beam, sensor segmentation choice, prototype structure and plan for test beam measurements is presented.

Key words: ILC, Beam Calorimeter, GaAs, Test Beam

INTRODUCTION

The Forward region of future linear colliders can be instrumented by BeamCal. It is designed as 30 layers tungsten-sensor sandwich calorimeter instrumented by radiation hard sensors like Di or GaAs[1]. Located behind Luminosity calorimeter (LumiCal) it will surround two inclined beam pipes and require withstand high radiation doses. GaAs sensor planes were tested to be operational up to 1,5MGy.

Two of GaAs sectors were produced by Choralsky method and tested for IV and CV characteristics. Each sector is 500um thick, semi insulating GaAs substrate, annealed and metalized on both sides with Al or Ni. One of the metallization sides is divided by 12 rings, and each ring in squares of different areas, see Table 1. Fig. 1 show example of segmentation called proportional. Pad sizes are increasing proportional to radius number.

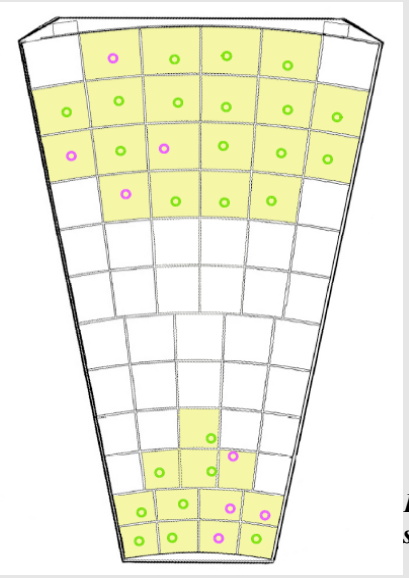

Figure 1. GaAs sector with proportional segmentation

SIMULATION

Radiation hardness is a strong requirement for BeamCal sensors due to beamstrahlung e+e- pairs on small polar angles expected on future e+e- linear colliders. On the Fig.2 (left) shown simulation of one bunch crossing deposited energy in one of two BeamCal's sensitive layers. Segmentation is chosen to be squared. It is shown, that there is higher deposited energy in smaller radii. Fig.2 (right) shows second segmentation, radial increasing and with proportionally squared pad areas. One of the BeamCal goals is to make detector system hermetic or detect single high energetic electrons or positrons (sHEe) escaping at small polar angles[2]. In the BeamCal sHEe will cause electromagnetic shower with Moliere radius ~11mm estimated by GEANT4 simulation.

Table 1. Comparison of two GaAs sectors

Value	Sensor 1	Sensor 2
Metallization	Al	Ni
Pads	87	64
Sector angle	45^0	$22{,}5^0$
Inner radius	20mm	84 mm
Outer radius	48 mm	114 mm
Pad area	~25 mm^2	16- 42 mm^2

For studying sensor segmentation influence on electrons reconstruction simulation by GEANT4 was done. On the Fig. 2 shown square segmentation and one bunch crossing of 500Gev with nominal ILC beam parameters [3] and one 250GeV electron shower overlapped. It can be seen on top of background of e+e- beamstrahlung pairs. The shower has narrow core. For calculation of the single electron reconstruction efficiency on top of huge background special algorithm was implemented [4]. And on Fig. 3 shown comparison between efficiencies of electron shower reconstruction for two segmentations. Square segmentation has pads of equal sizes ~8x8 mm^2 and proportional segmentation has pads of various sizes. Energy of primary particle was set to 150 GeV. Fig. 3 shows increase of reconstruction efficiency for proportional segmentation. By reducing size of the inner pads and shower core independent from segmentation of BeamCal sensors, reconstruction efficiency can be improved.

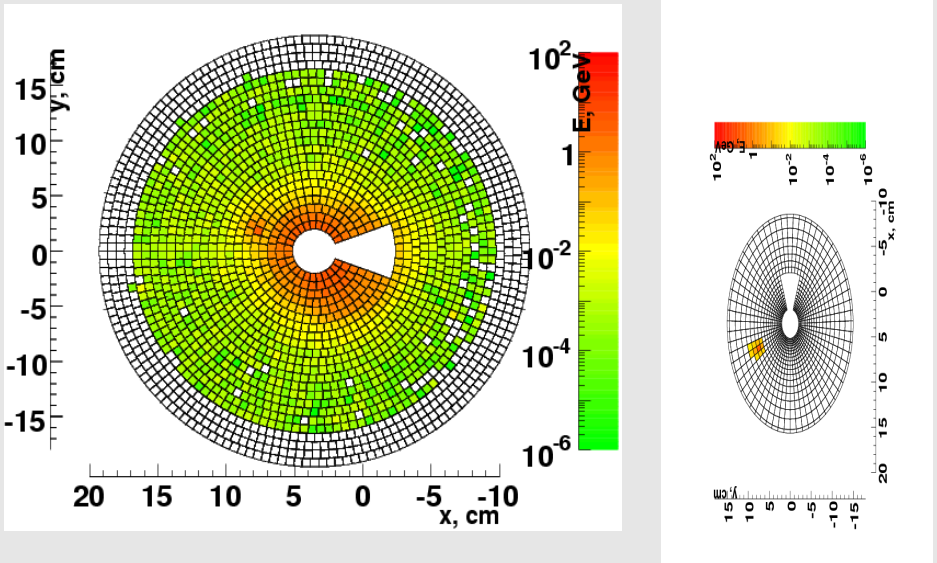

Figure 2. Full deposited energy in BeamCal sensor layers of one bunch crossing and square segmentation (left) and proportional segmentation (right).

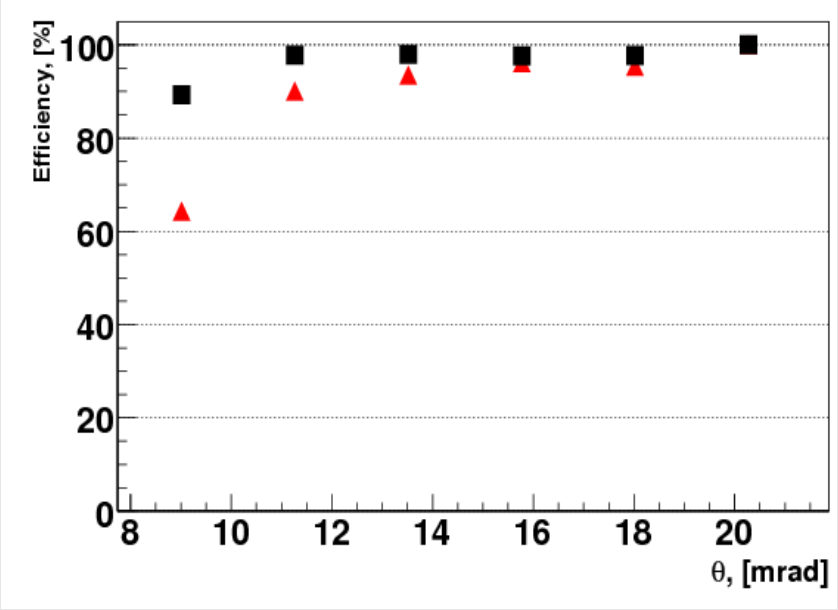

Figure 3. BeamCal electrons reconstruction efficiency for 150 GeV electrons, square segmentation (triangles) and proportional segmentation (squares).

SECTOR CHARACTERIZATION

There were 11 GaAs sectors produced with proportional segmentation and all were characterized for current voltage characteristics (I-V) and capacitance voltage characteristics (C-V) for each pad of sector. Sensor sectors have similar structure as proportional segmentation used for simulation with pads size varying from 25 to 40 mm^2. It allowed checking capacitance dependence versus pad area and comparison with parallel plate capacitor formula.

Capacitance is measured in probe station with LCR-Meter applied by connecting to the pads with needles. As shown on Fig. 4 all measured capacitances for one sector are laying on the line and have a shift in 5 pF in comparison to the calculated values. This effect can be explained by nonlinearities at the edges due to one side fully metalized. Fig. 5 presents capacitances of AG221-25 GaAs sensor for each pad as a function of pad number and sorted by rings. Small decrease of capacitances on the sides is explained by smaller pads size due to guard ring.

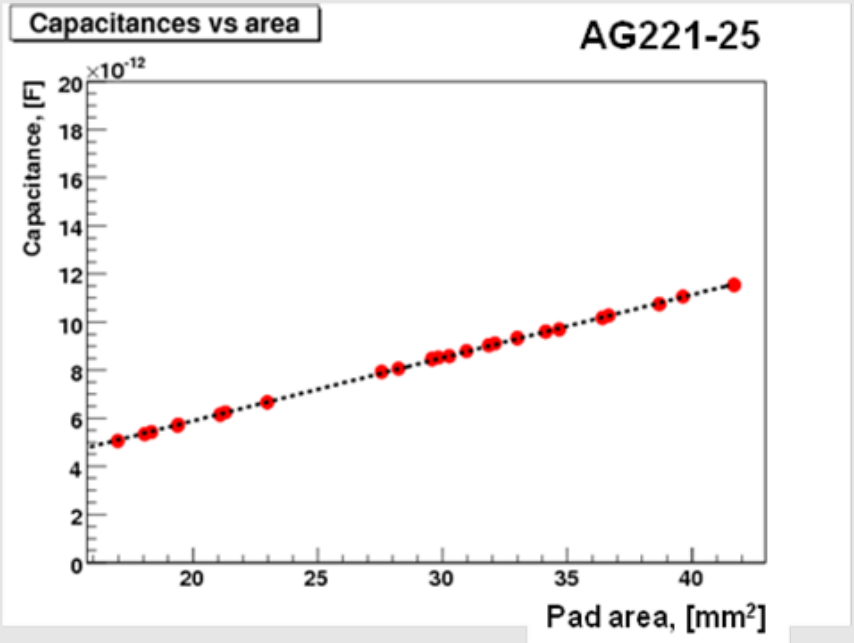

Figure 4. Capacitances of AG221-25 GaAs sensor plane with proportional segmentation as a dependence of pads area.

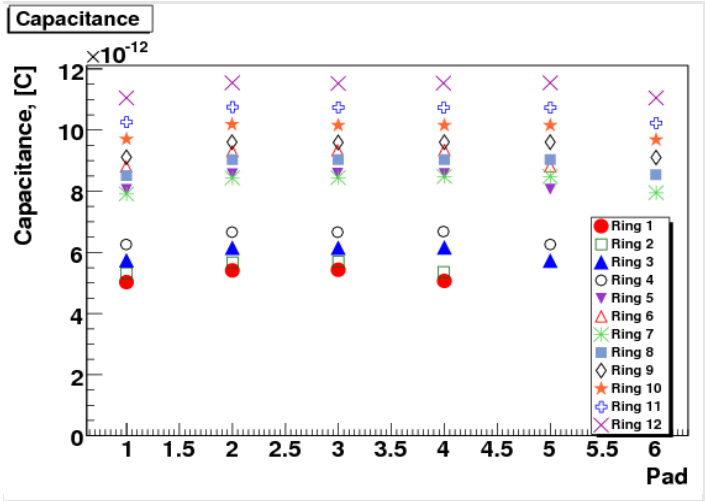

Figure 5. Capacitances of AG221-25 GaAs sensor plane with proportional segmentation versus pad number for different rings.

TEST BEAM PLAN

Planning test beam has two main aims: to operate full BeamCal prototype (GaAs sector, fan-out, ASIC's. ADC's) and full system characterization: signal to noise ratio, amplitude and charge spectra measurements, charge collection efficiency, cross-talk, temperature dependence measurements and edge investigations for new type of metallization segmentation. Option of monitoring and measure signals with external flash ADC CAEN 1721 was kept.

Read out board prepared by AGH in Krakow with prepared DAQ are used for data taking. R/O board contain: sensor board connector (SAMTEC-SFMH-145-02-L-D-LC), 4 front-end ASICs, 4 8-channel 10bit ADC, FPGA for DAQ (Xilinx Spartan) and microcontroller (Atmel AVR ATXMEGA128) [5]. Sensor AG221-25 was chosen by C-V and I-V optimal measured values. It was glued to the prepared thin PCB fan-out with traces to pads marked on Fig. 1 and shown on both sides on Fig. 6. All together 32 pads were bonded to the fan-out. Fan-out was instrumented by 10 nF capacitances and 1 MΩ resistors. Then it was connected to 90-way, 2-row J2 connector (FSH-145-04-L-RA-SL).

Test beam is planned to be in DESY II ring in November 2011.

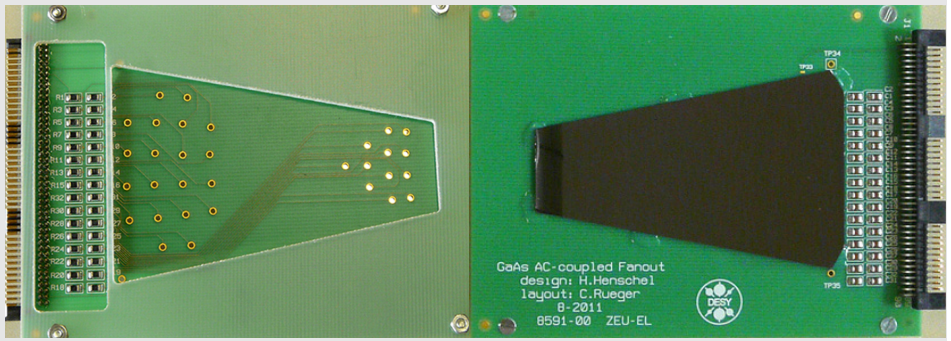

Figure 6. Sensor mounted on fan-out and instrumented by capacitances, resistors and connector.

REFERENCES

[1] V.B. Chmill at.al., An exploration of GaAs structures for solid-state detectors, Nuclear Instruments and Methods m Physics Research A326 (1993) 310-312

[2] The International Large Detector: Letter of Intent, arXiv:1006.3396v1

[3] ILC beam parameters, http://ilcphys.kek.jp/soft/ILCBeam/index.html

[4] O. Novgporodova, Studies on the Electron Reconstruction Efficiency for the Beam Calorimeter of an ILC Detector, Proceedings, LCWS/ILC2010

[5] M. Idzik, S. Kulis and D. Przyborowski , Nucl. Instr. and Meth. A 608 (2009) 169

ANALYSIS OF LUMICAL DATA FROM THE 2010 TESTBEAM

By

Itamar LEVY[1]

(4) *Tel Aviv University, School of Physics and Astronomy, Tel Aviv, Israel*

This paper summarizes some new analyses of the first data taken with the LumiCal sensor prototype and the ZEUS MVD telescope in the test beam at DESY by the FCAL collaboration in the summer of 2010. Spectrum-analysis and cross-talk estimation are shown here. Also presented is the analysis of signal dependence on the position in the sensor.

Key words: FCAL,LumiCal,TestBeam

INTRODUCTION

In the summer of 2010 the FCAL collaboration performed the first test-beam measurements of the Lumical silicon - and the BeamCal GaAs-sensors prototype [1,2].

In these measurements, the full readout chain, including silicon sensors, Kapton fan-out and front-end electronics [3], were tested. The test beam was performed at DESY-II area 22, using 4.5 GeV electrons [4].

This paper will summarize some results of new analyses made of the LumiCal 2010 test-beam data. These results include spectrum and cross-talk analysis, and combinations between sensor and position-reconstruction data.

TEST BEAM SETUP

For the track-measurement of each beam- particle the ZEUS MVD telescope [5] was used. It consists of three modules, each containing two perpendicular layers of silicon strip detectors. Hence, each module provides x, y and z coordinates which can be used for track reconstruction to predict the hit-position in the device under test (DUT).

Each layer of silicon is a single-sided silicon-strip detector, 300 μm thick and 32 mm x 32 mm in area. The strip pitch is of 25 μm and the read-out pitch of 50 μm.

To study the performance of the sensor plane as a function of position, the sensor box (DUT) was put between the second and the third planes of the ZEUS telescope as shown in Fig. 1.

The DUT was set up on a remotely-controlled precision x-y table, which allowed the DUT to be moved in the beam. The x-y table itself was mounted on the same optical bench as the telescope.

The sensor tile was bonded to a Kapton fan-out that delivered signals to the front-end electronics on the attached PCB. The analogue signals from the front-end electronics were driven out of the box and sent to an external sampling ADC (v1724, 14 bit, 100 Msp/s) provided by CAEN.

As shown in Fig. 1, three scintillators followed by photomultipliers working in coincidence were providing triggers for both the telescope and the LumiCal data acquisition systems (DAQ). A veto scheme (through BUSY signal) was used to ensure that both DAQs acquired the same number of events.

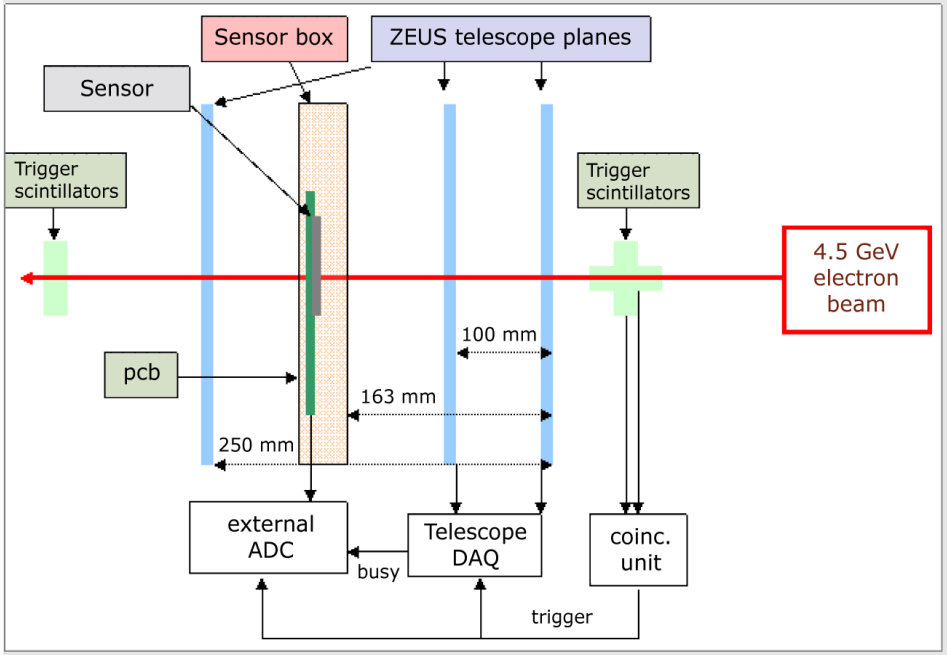

Figure 1. Test beam setup and connection scheme.

SPECTRUM ANALYSIS

Two areas of the silicon sensor have been measured, 8 pads at the outermost radius of sector L1 (area 1) and 8 pads at the innermost radius of sector L2 (area 2) as shown in Fig. 2. Since the beam profile is 5mm x 5mm, 20 measured-points and around 1M triggers were collected for each area. At trigger time all 8 channels were recorded, with 128 sample points 10ns apart, as shown in Fig.3.

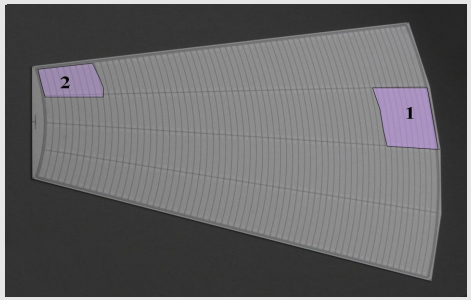

Figure 2. Tail of the silicon sensor prototype. Measured areas (1 and 2) are highlighted.

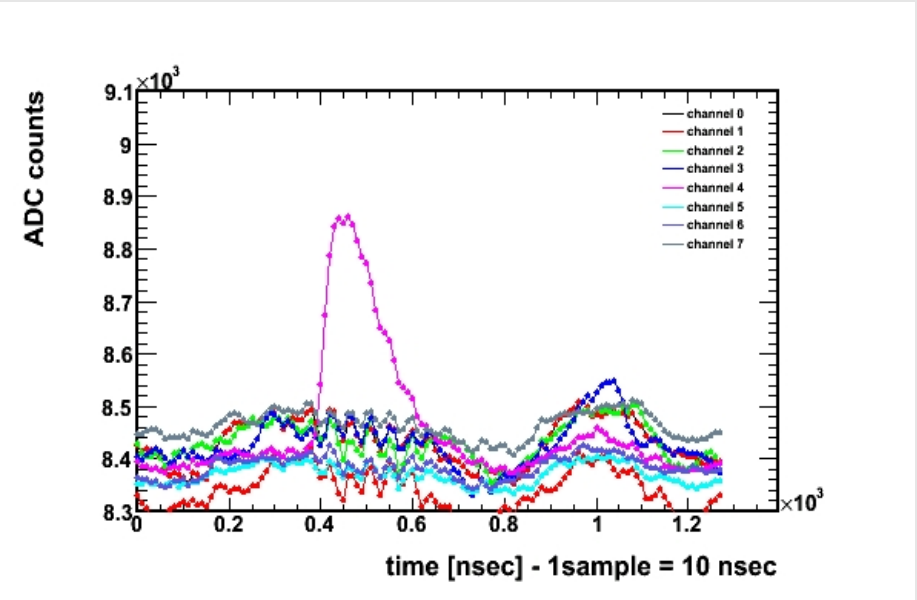

Figure 3. A full event as recorded in the v1724 ADC.

From a comparison of the level of noise around the average

level of base-line in all channels, noise correlation between channels is observed. In order to estimate the correlation coefficient between every two channels, one can use in empty events the following definition:

$$\rho = \frac{\langle S_i S_j \rangle - \langle S_i \rangle \langle S_j \rangle}{\sigma_i \sigma_j}$$

where S_i is the sample and σ_i is the RMS of the 128 samples in channel i in an event. For each pair of channels we determined the correlation coefficient for all empty events. The most probable value (MPV) of the correlation coefficient between all sets of channels was of the order of 0.7.

The high correlation coefficient indicates a common-mode noise between channels. This noise comes from the front-end electronics. To reduce the common-mode noise one should apply a filter. In our filter we first subtract the average baseline for each channel from the signal and then we average-out the common-mode noise over all channels in one event.

When subtracting the baseline, one needs to take into account the baseline dependence on temperature. In the pads of area 2, observe temperature differences of ~20ADC counts per 1 °C for all channels.

To analyze the spectrum, integration within the 40nsec and 100nsec windows were done for all channels in all events. To complete the measurement, the spectrum was fitted by a Gauss-Landau convolution as seen in Fig. 4. For each channel, we define the signal-to-noise, S/N, as

$$S/N = \frac{(MPV)_{signal} - \langle mean \rangle_{padestal}}{\langle \sigma \rangle_{padestal}}$$

After applying the common mode filters on the signals, the S/N increases from below 10 to 30 – 45, depending on the channel gain. The results for the same measurement using only the maximum amplitude for each event, yield even higher S/N values. Without filtering, the S/N reaches values of ~20 and after filtering, the S/N values rise to above 60.

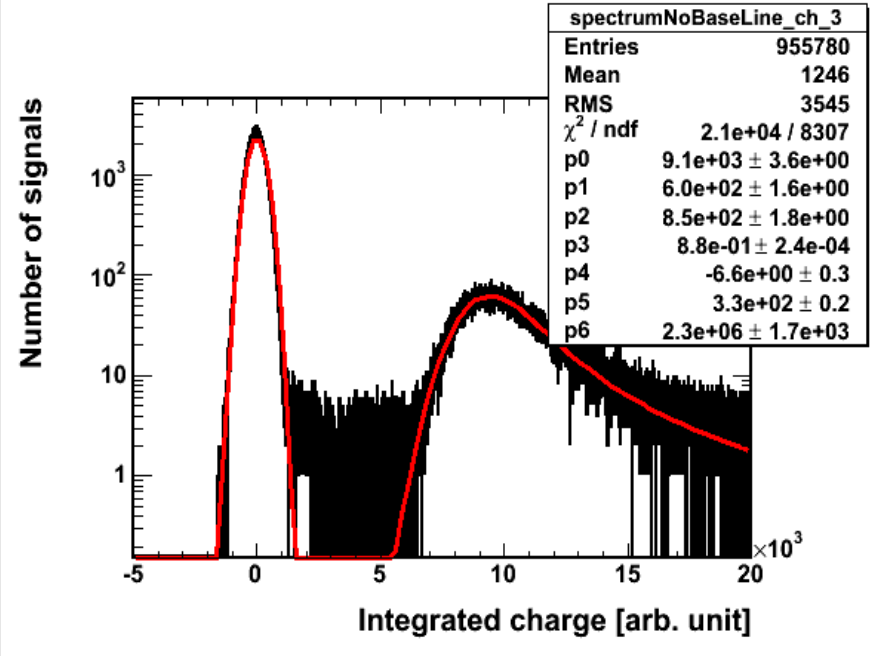

Figure 4. An example of the spectrum after applying filter.

CROSS-TALK

In an attempt to investigate the correlation between channels and the cross-talk, we made a point-by-point 2D correlation graph

for each pair of channels. An example is shown in Fig. 5.

We try to estimate cross-talk coefficient by using the ROOT profile tool, and study the behavior of the mean value of the pedestal as function of signal size in the other channel.

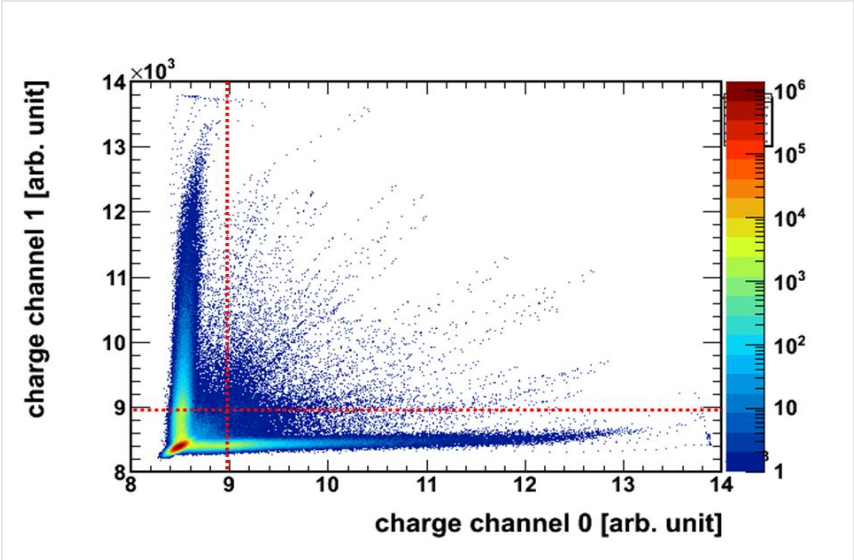

Figure 5. Point-by-point 2D correlation plot. The significant area of cross-talk is estimated between the outer x-y axes (black) and inner axes (red).

We define the cross-talk coefficient as the slope of the profile graph, normalized by the ratio between the MPV amplitude of each channel. As expected, the cross-talk coefficient, seen in Fig. 6, is low and is relevant only in neighboring channels. We observed that the cross-talk coefficient of pads in area 2 (~3%) is more than twice the coefficient in the pads of area 1 (~1%). We can estimate that this is due to the long transition-lines from pads in area 2 to the ASICs locate in the radial direction after the edge of the sensor.

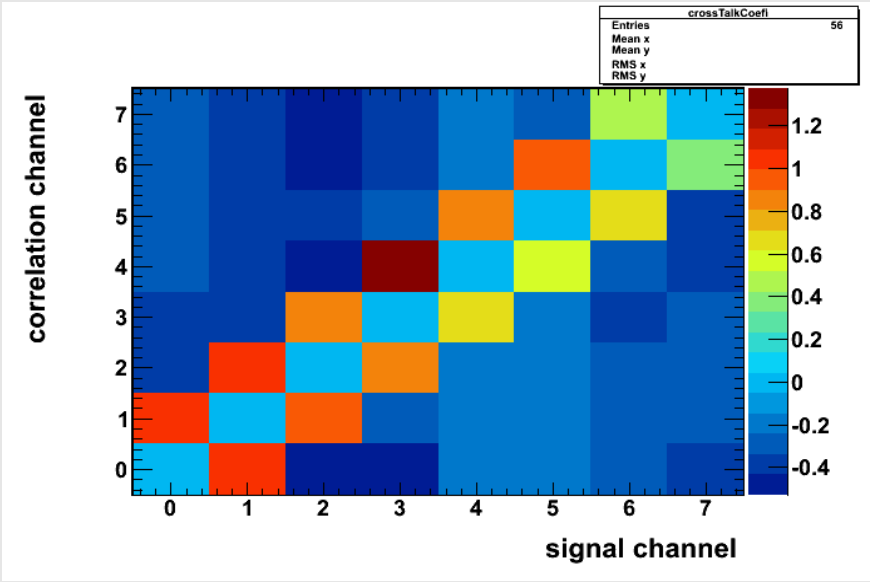

Figure 6. Cross-talk coefficient map of pads in area 1.

POSITION RECONSTRUCTION & CHARGE COLLECTION

In this test-beam, the time stamping was critical since one needs to match between events in the sensor tile and in the telescope. We rely on the trigger/busy logic and low rate of events at 4.5 GeV to determine that the two systems have the same number of events. Then, by shifts in small number of events, one can match and use all the information of an event.

Position reconstruction was made by fitting a linear line to the position recorded by the telescope in each plane. To ensure the track accuracy, only tracks with one hit per plane and three hits in the telescope were reconstructed. This reduced the reconstruction

efficiency to ~50\%. In Fig. 7, the position reconstructed on the sensor surface is shown. Each hit is represented by a color according to the channel that had a signal higher than the threshold.

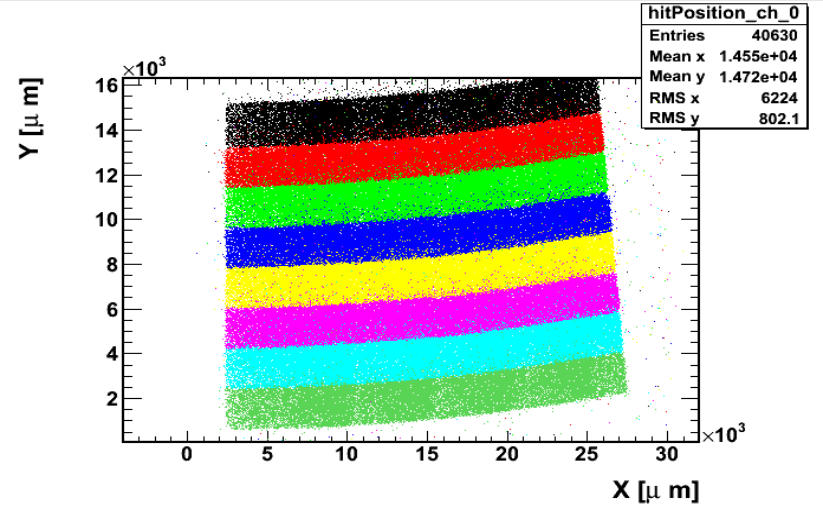

Figure 7. A map of hits in the sensor area. The color is attributed according to the channel in which a signal was obseved.

The response of the sensor was studied as a function of the position of the beam relative to the sensor. The average charge per channel, divided by the MPV of the charges in that channel, is shown in Fig. 8. In general, the charge collection is uniform. A decrease of charge collection of about 10% is observed in the region of ±0.1 mm around the location of the 0.1 mm gap between pads.

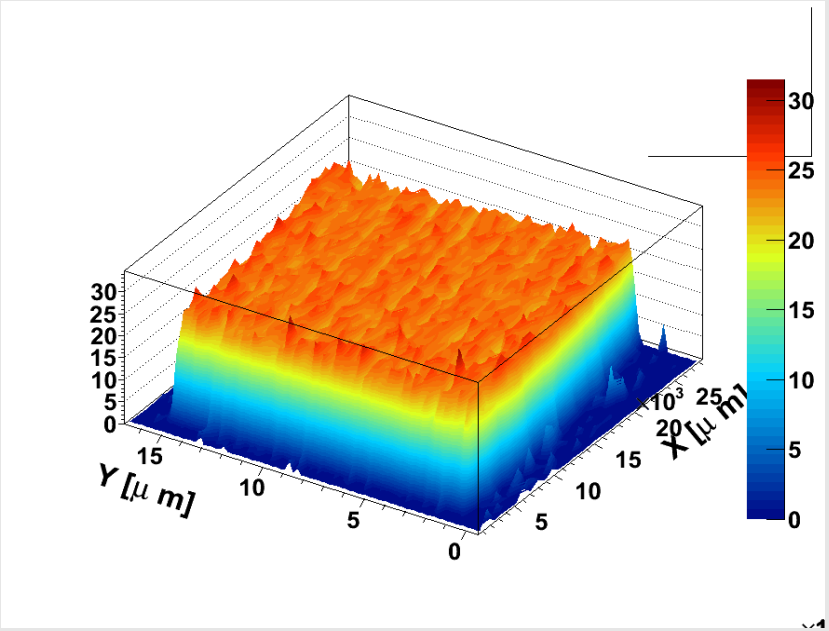

Figure 8. The average signal divided by the MPV as a function of hit position.

SUMMARY

This paper summarizes some new results obtained with the first data taken with the LumiCal tile prototype in the test beam at DESY in the summer of 2010. In the data, a high correlation coefficient is observed between signals of all channels. These correlations are due to the common-mode noise in the ASICs. When calculating the S/N ratio, by integrating or by using the maximum amplitude, reasonable values are achieved that improve dramatically when filtering-out the common-mode from the data.

The test-beam data show that the baseline of the signal has temperature dependence of ~20 ADC count per 1°C. This effect needs to be taken into account when analyzing large parts of data.

We use point-to-point 2D correlation plots between sets of channels to estimate the correlation between them. By inspecting the change of the mean value of the pedestal of one channel as a function of the whole spectrum in the other one, a cross-talk estimation can be obtained. Using this method we were able to evaluate cross-talk of neighboring channels as 1% for pads in area 1 and 3% for pads in area 2. This difference suggests that the main contribution comes from the length of transition lines.

First measurements of the signal dependence on the position in the sensor shows uniformity between pads and in pad domains. It also shows a decrease of 10% - 20% in the area of the gaps between pads, but further study is needed.

ACKNOWLEDGMENTS

This work was partly supported by the Israel Science Foundation.

REFERENCES

[1] S. Kulis et al., *Test beam studies of the LumiCal prototype*, Eudet-Memo-2010-09.

[2] O. Novgorodova et al., *Forward Calorimeters for the Future Electron-Positron Linear Collider Detectors*, PoS QFTHEP (2010) 030.

[3] M. Idzik, S. Kulis and D. Przyborowski, *Development of front-end electronics for the luminosity detector at ILC*, Nucl. Instrum. Meth. **A 608** (2009) 169.

[4] Test beam facility at DESY,

http://adweb.desy.de/~testbeam/

REPORT ON FCAL COLLABORATION TESTBEAM

By

Sz. KULIS[1]*, A. MATOGA[1], J. AGUILAR[1,2], I. LEVY[3], L. ZAWIEJSKI[2], E. KIELAR[2], O. NOVGORODOVA[4], H. HENSCHEL[4], I. SMILJANIĆ[5], W. WIERBA[2], J. KOTULA[2], A. MOSZCZYNSKI[2], K. OLIWA[2] AND W. DANILUK[2]

(1) University of Science and Technology, AGH, Cracow, Poland

(2) Institute of Nuclear Physics, PAN, Cracow, Poland

(3) Tel-Aviv University, YAU, Tel-Aviv, Israel

(4) Deutsches Elekronen-Synchrotron, DESY, Zeuthen, Germany

(5) Vinca Institute of Nuclear Sciences, Belgrade, Serbia

A prototype of a LumiCal sensor module was designed and successfully tested on the 4.5 GeV electron beam (DESY II,Hamburg). Full chain is composed of silicon sensor, kapton fan-out, dedicated front-end and ADC ASICs and FPGA based data concentrator. Some very preliminary results, confirming proper system operation, are presented and discussed.

Key words: Detector module, silicon sensor, front-end, ADC, FPGA, DAQ, testbeam.

INTRODUCTION

The precise measurement of the luminosity at future linear colliders will be done by special detector, LumiCal, placed in very forward region[1]. A design studies are being performed for International Linear Collider (ILC) [2] and Compact Linear Collider (CLIC) [3]. The complete Lumical [4] detector contains two electromagnetic calorimeters placed on both side of the interaction point. The single calorimeter contains 30/40 (ILC/CLIC) layers of tungsten absorber interspersed with silicon sensor planes. The sensor layers are segmented radially and azimuthally into pads of different sizes. Signals from sensor are amplified, shaped and digitized in dedicated, fast and low-noise readout electronic. A most recent design of the LumiCal internal structure was included in [5].

The readout concept for each experiments is different, mostly due to different beam structure. In ILC bunch crossing will happen every 330 ns, giving a plenty of time for processing each event separately. Signal from the event is amplified by charge sensitive preamplifier and processed by fast CR-RC shaper (60 ns peaking time) and one ADC conversion is done for pulse maximum. In CLIC period between subsequent bunch crossings is at 0.5 ns level, resulting beam being almost continuous from electronic point of view. An attractive readout scheme for such environments may be to use only one analog processing chain with a relatively fast Analog to Digital Converter (ADC) incorporated in each channel. Taking an advantage of having digital samples, one may think about variety of algorithms to extract information about time and amplitude of events which can not easily be applied using analog technology [6].

To verify proposed readout scheme a test beam measurements took a place in July 2011 in *Deutsches Elektronen-Synchrotron Research Centre (DESY) Hamburg. Complete multichannel detector module is comprised of silicon sensors, kapton fanout, front-end ASICs (32 channels) multichannel

ADC SoC ASICs (32 channels), data concentrator implemented in Field Programmable Gate Array (FPGA) as well as a digitally controlled and monitored biasing and powering circuits.

The paper is organized in two parts. In the first part the experimental setup and design of prototype module are presented. The second part discusses the preliminary results of measurements.

Finally, brief conclusions and plans for future work are given.

EXPERIMENTAL SETUP

The beam test measurements took place in the July 2011 at DESY-II area 22 [9]. A bremsstrahlung beam was generated by a carbon fibre in the circulating beam of the electron/positron synchrotron DESY II. The photons were converted to electron/positron pairs with a metal plate (converter). Then the beam was spread out with a dipole magnet. The final electron beam is cut out with a collimator. For presented below measurements, electrons with 4.5 GeV energy were picked up. Schematic diagram of experimental setup is presented in Figure 1. The track of each beam particle was measured by the MVD ZEUS telescope. It consists of three planes. Each plane contains two perpendicular silicon strip detectors. Combining signals from both sensors x, y impact position may be found. Using information form all planes impact position on device under test (DUT) plane may be predicted [10].

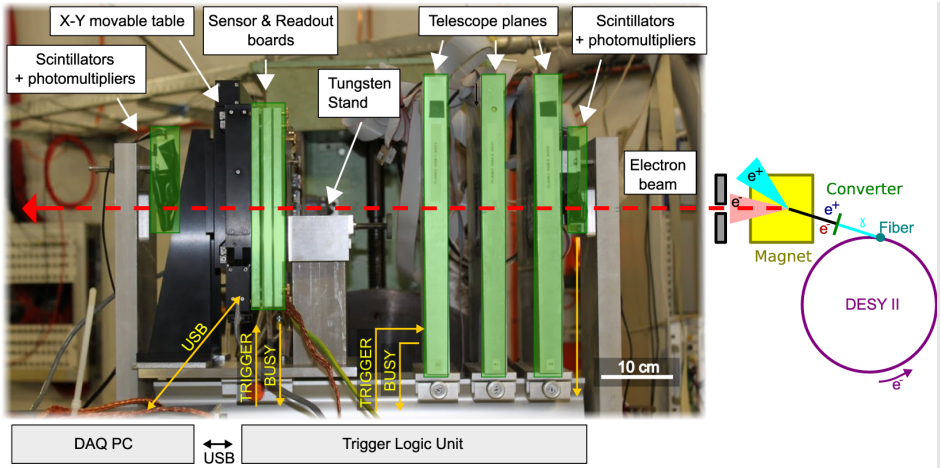

Figure 1. Schematic diagram of experimental setup.

The DUT was mounted on remotely controlled, motorized X-Y translation stage. It allowed to change electron impact point on sensor plane.

Trigger signal for all subdetectors (MVD telescope, DUT) was generated by Trigger Logic Unit (TLU) [13] based on signals from three scintillators (two in front of telescope and one after DUT) followed by photomultipliers. The EUDAQ portable DAQ Software framework [12] was used for data taking and event building.

READOUT SYSTEM

The block diagram of developed detector module [8] prototype is presented in Figure 2. The module is composed of two Printed Circuit Boards (PCB), namely sensor and readout boards. Splitting module allows different kinds of sensors to be connected to one

* Corresponding author

readout. Kapton fanout is glued on top of sensor and signal tracks are wire bonded to it. A second end of kapton tracks are wire bonded to PCB and then routed to multiway connector.

Only 32 biggest pads, on top of sensor tail, are read out by front-end electronics, while the rest of pads are grounded. The signal is amplified and shaped using dedicated front-end ASICs [11], and digitized in pipeline ADC chips, working continuously with sampling rate of 20 Msps. The data stream leaving the ADC is continuously written into a buffer inside FPGA.When the trigger occurs, the microcontroller firmware builds event packet and transmits it to PC. Currently Universal Serial Bus (USB) is used as a communication interface. However module is foreseen to support interface to Link Data Agregator (LDA) which suppose to be a common part for all ILC subdetectos [7].

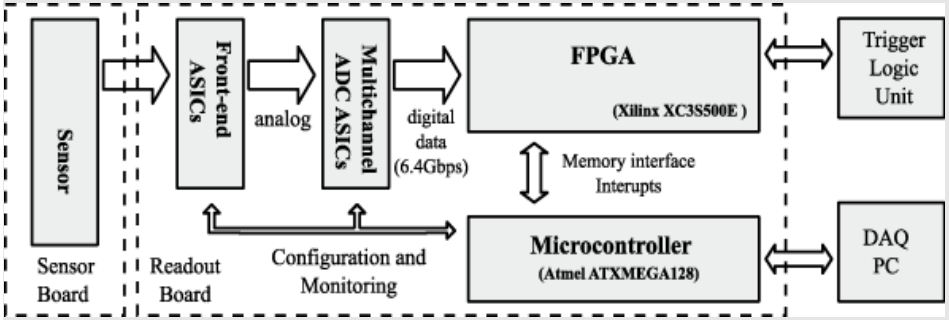

Figure 2. Readout system block diagram.

MEASUREMENTS RESULTS

To evaluate system performance a set of measurements was taken. During testbeam system was working asynchronously with beam. To recover information about event's amplitude a deconvolution method was applied [6]. Example spectrum of energy deposited in one pad is presented in figure 3. Measured data points (in red) fit very well to Landau convoluted with Gauss distribution (blue). Signal to noise ratio (SNR), calculated as mean probable value (MPV) of Landau distribution to RMS of baseline, was find to be grater than 20 for each channel.

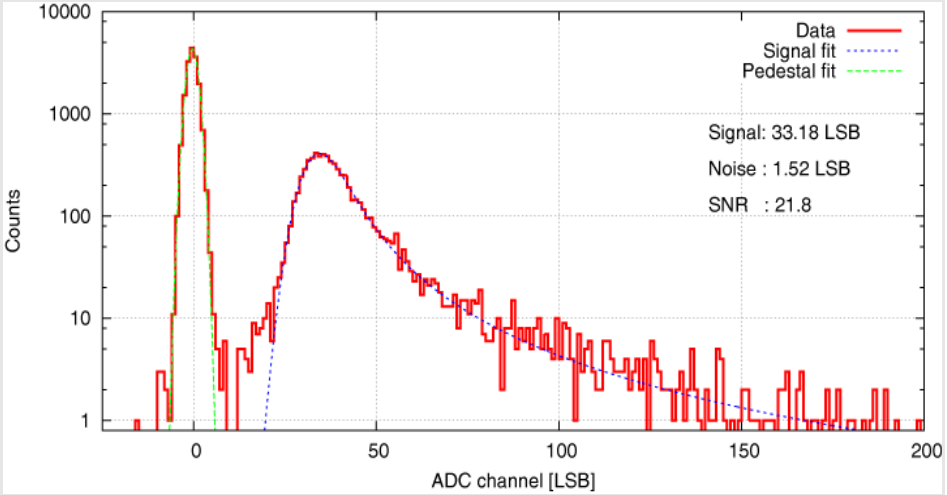

Figure 3. Energy deposition spectrum for single electron events collected from one channel.

In the next step response of detector to electromagnetic shower was studied. Figure 4 shows the histogram of energy deposited in the whole instrumented area (signal integrated over 32 pads) after passing through one 3.5 mm thick tungsten plate, what corresponds to one radiation length.

In zoomed part of beginning of the spectrum signal corresponding to 1 or 2 electrons can be observed.

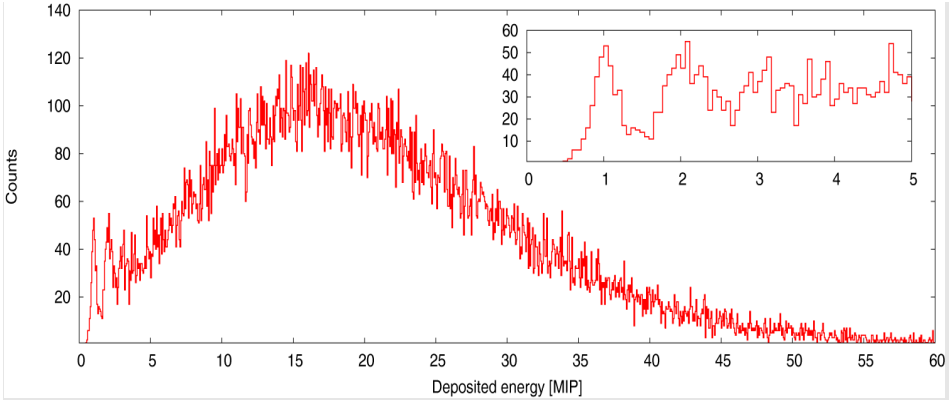

Figure 4. Integrated energy depositied on whole instrumented area with one tungsten plate in front of sensor plane.

Same analyzes were performed for different thickness of tungsten absorber. An average charge deposited in whole instrumented area as a function of tungsten absorber thickness is presented in Figure 5a. Electromagnetic cascade for 4.5 GeV electrons has its maximum after 5 radiation lengths. More detail charge deposition distribution, as a function of lateral shower width and absorber thickness is shown in Figure 5b. More detailed analyzes as well as Monte Carlo simulations of described system are being performed right now.

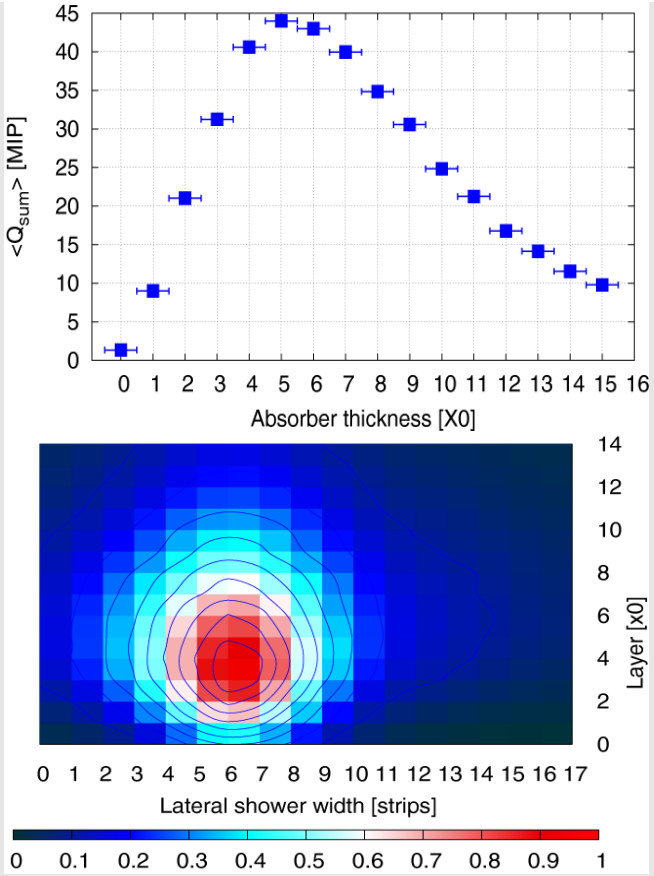

Figure 5. (a) Average charge deposited in whole instrumented area as a function of tungsten absorber thickness; (b) Energy deposited in one sensor strip for different tungsten absorber thickness normalized to maximum deposition .

SUMMARY & FUTURE WORK

The set of measurements, performed at electron beam at DESY, confirmed proper operation of fully assembled detector module. The obtained results indicate a good working performance of all components, namely: silicon sensors, kapton fanout and front-end, analog to digital converter as well as data concentrator unit. Test beam measurements allowed also the studies of shower development using tungsten as an absorber. The developed multichannel readout system will be extensively used in test beams and laboratory studies of ILC/CLIC readout schemes. It should be integrated to Common DAQ.

ACKNOWLEDGMENTS

This work was supported by the Commission of the European Communities under the 7th Framework Programmes: “Marie Curie ITN”, MC-PAD grant agreement number 214560, and Advanced European Infrastructures for Detectors and Accelerators, AIDA grant agreement number 262025. This work was also supported by the Polish Ministry of Science and Higher Education and its grants for Scientific Research. The authors would like to thank DESY providing test beam time.

REFERENCES

[1] The Internatonal Large Detector, Letter of Intent, February 2010, DESY 2009-87,FERMILAB-PUB-09-682-E; KEK Report 2009-6.

[2] International Linear Collider, http://www.linearcollider.org/.

[3] Compact Linear Collider, http://clic-study.org/.

[4] The FCAL Collaboration, http://www-zeuthen.desy.de/ILC/fcal.

[5] H. Abramowicz et al., Forward instrumentation for ILC detectors, JINST 5 (2010) P12002.

[6] Szymon Kulis, Marek Idzik, Study of readout architectures for triggerless high event rate detectors at
CLIC LCD-Note-2011-015

[7] V. Bartsch, Status of the CALICE DAQ system LCWS08 conference proceedings

[8] A. Matoga Prototype readout system for beamtest of ILC forward calorimetry detector modules
Proceedings of the 18th FCAL Collaboration Workshop, 2011, Predeal, Romania

[9] D.Autiero, P.Migliozzi et.al., OPERA Collaboration, Characterization of the T24 electron beam line available at DESY, March 12, 2004

[10] I. Gregor, http://www.desy.de/˜gregor/MVD_Telescope.

[11] M. Idzik, Sz. Kulis, D. Przyborowski, Development of front-end electronics for the luminoisty detector at LC, Nucl. Instr. and Meth. A, vol. 608, pp.169–174, 2009.

[12] E.Corrin EUDAQ Software User Manual, Eudet-Memo-2010-01

[13] D. Cussans Description of the JRA1 Trigger Logic Unit (TLU), v0.2c, EUDET-Memo-2009-4

STATUS OF LUMICAL READOUT ELECTRONICS

By

M. IDZIK[1]

(1) University of Science and Technology, AGH, Cracow, Poland

The development status of readout electronics for LumiCal detector at future linear colliders is presented. The dedicated front-end and digitizer ASICs designed and fabricated for this purpose are briefly presented. The prototype of the whole chain of the LumiCal readout module, comprising the sensor, the readout ASICs and the FPGA based data concentrator is described.

Key words: Detector module, silicon sensor, front-end, ADC, FPGA, DAQ, testbeam.

LUMICAL READOUT ARCHITECTURE

In last few years the works on readout architecture comprising a dedicated front-end and and a dedicated ADC in each readout channel were carried. The idea was to build a readout chain consisting of two dedicated ASICs (FE, ADC) and to complete it with FPGA based data concentrator. The block diagram of the developed readout architecture is presented in Figure 1. The signal from a sensor is amplified and shaped in a dedicated multichannel front-end ASIC, and digitized in a dedicated multichannel digitizer ASIC, continuously sampling the front-end output. The digitized data stream is continuously recorded and processed in a Field Programmable Gate Array (FPGA) and sent to the host PC.

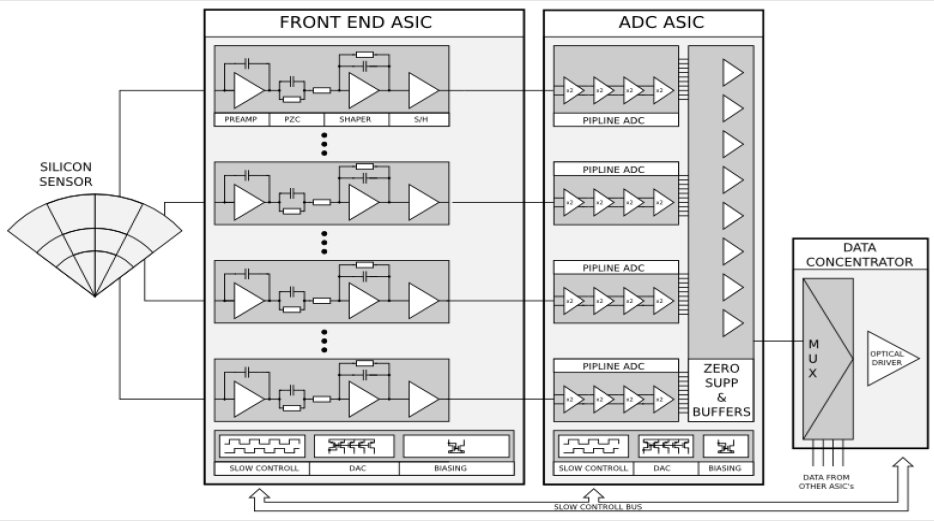

Figure 1. Schematic diagram of experimental setup.

FRONT-END

The developed front-end ASIC architecture [1] comprises a charge sensitive preamplifier, a pole-zero cancellation circuit (PZC) and a CR-RC shaper (Figure 2). The 60 ns peaking time of the shaper together with the PZC, which cancels the elongated response of the preamplifier, make the whole pulse to fit in about 350 ns. This allows for high hit rate of about 3 M events per second, which may be further increased by using digital signal processing. In order to cope with large charges in the physics mode and the

small ones in the calibration mode a variable gain in both the charge amplifier and the shaper is applied. In the high gain, low noise, mode it is able to detect signals from below 1 fC to about 30 fC, while in the low gain mode it is capable of measuring high charge depositions exceeding 10 pC per channel. The front-end works with a wide range of sensor capacitances, up to above 100 pF.

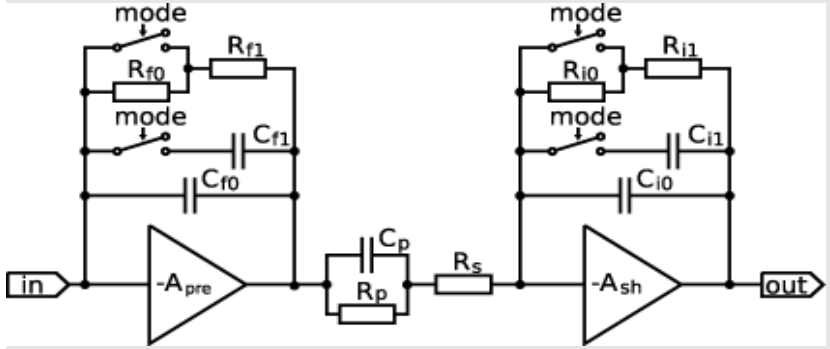

Figure 2. Block diagram of a single front–end channel.

The prototype ASIC was fabricated in a 0.35 μm, four-metal two-poly CMOS technology. The photograph of prototype ASIC glued and bonded on the PCB is shown on Fig. 3. The ASIC contains 8 front-end channels.

Each channel consumes about 8.9 mW, in agreement with the performed simulations. The functionality and the essential parameters like gain, noise, high counting rate, crosstalk, were measured confirming the expected performance [1].

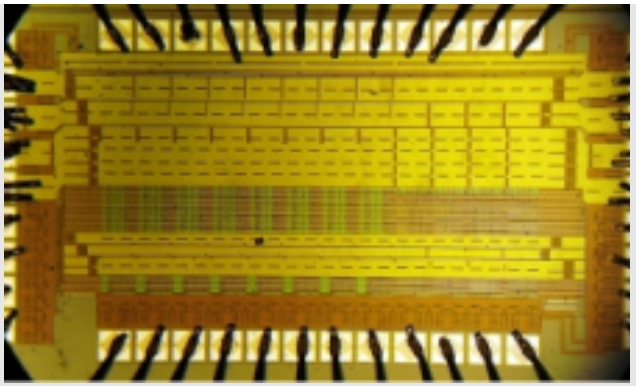

Figure 3. Photograph of glued and bonded front-end ASIC prototype.

MULTICHANNEL ADC

The multichannel digitizer ASIC contains 8 fully differential, power scalable 10-bit pipeline ADCs [2], a digital serializer allowing partial (10 bits to one output) or full (8 channels times 10 bits to one output) serialization, a fast LVDS I/O interface, a bandgap voltage reference, a proportional to absolute temperature (PTAT) temperature sensor, a set of built-in biasing DACs, and a digital control unit. It works for sampling rates from about 10 kSps to 25 MSps. The measured efective resolution is 9.7 bits.

To operate with maximum sampling rate the digitizer has to work in the partial serialization mode in which each ADC channel sends off the data using its own LVDS link (10 times faster than sampling frequency).

The prototype ASIC was fabricated in a 0.35 μm, four-metal two-poly CMOS technology. The micrograph of multichannel ADC prototype, glued and bonded on PCB is shown in Fig. 4. The active size of the ASIC is 3.17 mm × 2.59 mm. Eight ADC channels are

placed in parallel in 200 μm pitch and are followed by the serializer and LVDS pads, while the analog and digital peripheral circuits are on the ASIC sides. The meassured power consumption is of ~1.2mW/channel/MHz.

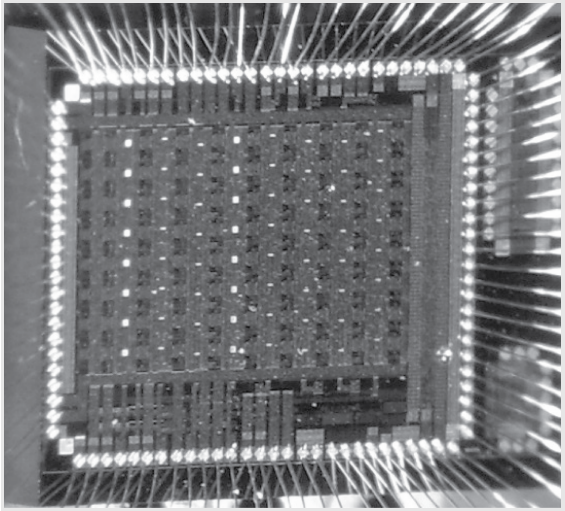

Figure 4. Micrograph of prototype ASIC bonded.

LUMICAL READOUT MODULE

Based on the developed readout ASICs a prototype of the whole LumiCal detector module comprising the sensor, the front-end, the digitizer, and the FPGA based data concentrator, was designed and built.

The prototype system was fabricated and assembled on 6 layer PCB. The photograph of assembled readout module is shown in Figure 5. In order to increase system flexibility and to allow operation with different sensors the signal is sent to front-end electronics through a multi-way connector.

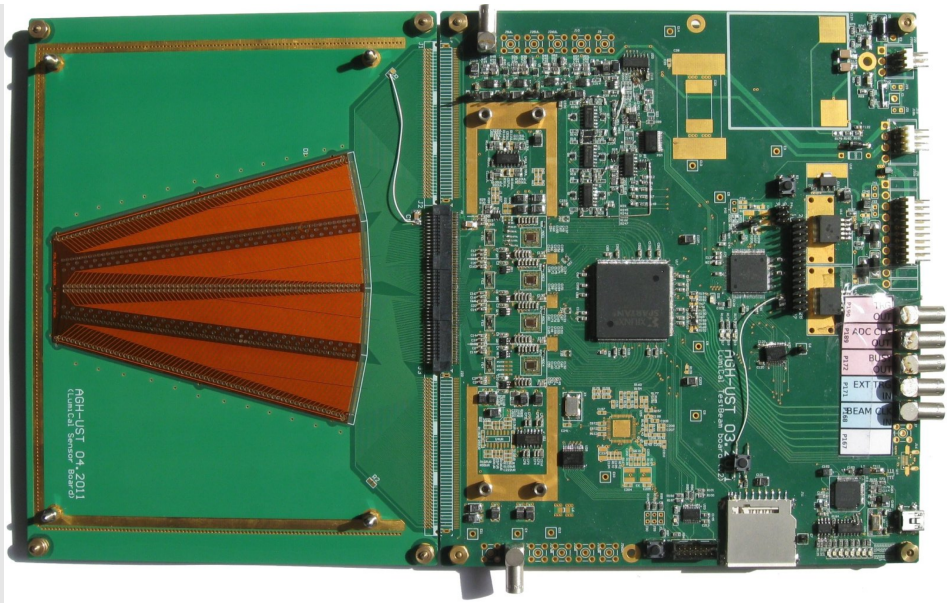

Figure 5. Photograph of readout system.

The signal is then amplified and shaped in the front-end ASICs, and digitized in the multichannel digitizer ASICs, continuously sampling the front-end output. There are four pairs of the front-end and digitizer ASICs, 8 channels each, giving 32 channels in total. Since the system was designed for testbeam use mainly to allow precise analysis of detector data, in particular the reconstruction of event amplitude and time and for pile-up studies, the main attention was given to ensure high enough ADC sampling rate and very high internal data throughput between the digitizer and the FPGA. The signal is sampled with 20 MSps rate, and digitized with 10-bit resolution, resulting in the raw data stream of about 6.4 Gbps. The digitized data stream is continuously recorded and processed in the Field Programmable Gate Array (FPGA). When a trigger condition

occurs, the acquisition is interrupted and microcontroller firmware builds an event packet and transmits it to a host PC.

To verify and to quantify the multichannel readout performance various measurements of different system sections and complete readout chain were done. The performed measurements showed the full system functionality. After the laboratory tests the module was succesfully used in the testbeams.

SUMMARY

The readout electronics ASICs for the LumiCal detector were developed, fabricated and tested. The protpotype multichannel module of the full readout chain comprising the sensor, the front-end, the digitizer, and the data concentrator, was built and tested. The measurements showed the excellent module performance, confirmed later by its operation during the testbeams.

ACKNOWLEDGMENTS

This work was supported by the Commission of the European Communities under the 7th Framework Programmes: “Marie Curie ITN”, MC-PAD grant agreement number 214560, and Advanced European Infrastructures for Detectors and Accelerators AIDA, grant agreement number 262025. This work was also supported by the Polish Ministry of Science and Higher Education and its grants for Scientific Research.

REFERENCES

[1] M. Idzik, Sz. Kulis, D. Przyborowski, Development of front-end electronics for the luminoisty detector at ILC, Nucl. Instr. and Meth. A, vol. 608, pp.169–174, 2009.

[2] M. Idzik, K. Swientek, T. Fiutowski, Sz. Kulis, P. Ambalathankandy A power scalable 10–bit pipeline ADC for Luminosity Detector at ILC, JINST 6 P01004 2011.

XY TABLE ISSUES

By

Jonathan AGUILAR

AGH University of Science and Technology, Department of Physics, Krakow, Poland

The two-dimensional motorized positioners used to control sensor position during beam tests of LumiCal and BeamCal prototypes have not performed satisfactorily. In the most recent test beam, the 8MTF-102 motorized XY positioner was unable to access its full range of motion in the vertical axis while bearing a load. The situation was reproduced in the lab, but a solution was unable to be found. After contact with the supplier, it was determined that the best course of action would be to send the table to the supplier for inspection and repair.

Key words: test beam, motorized positioner, x-y table

INTRODUCTION

The development of the luminosity and beam calorimeters, LumiCal and BeamCal respectively, for the ILC hinges on test beams in which prototypes of the calorimeter readout are tested in a low-energy (< 4.5 GeV) electron beam. The beam used is from the DESY II accelerator at DESY-Hamburg, which provides a beam a few millimeters in radius. In order to irradiate different parts of the LumiCal and BeamCal sensors, the sensors must be moved with high precision in the plane perpendicular to the beam direction.

Figure 1: A picture of the 8MTF-102 motorized positioner produced by Standa Ltd.

In previous test beams, we have used two different two-dimensional motorized positioners, with unsatisfactory results. During the first test beam, the sensor size was larger than the range of the motor. A decision was made by AGH to purchase a second motor with a greater range, which would also allow AGH to set up a sensor test bench in the lab, using a laser as the radiation source. The motor is rated up to a 6 kg load when placed in the vertical position. However, during the test beam, the motor failed to move vertically higher than about 60 mm as measured from the bottom of its range when loaded with two sensors and a tungsten plate,

totalling less than 4 kg. This paper details steps taken to characterize and resolve the problem.

POSITIONER DESCRIPTION

The motorized positioner is an 8MTF-102LS05 motorized XY scanning stage, produced by Standa, Ltd. of Vilnius, Lithuania. A picture is shown in Figure 1. It can travel 102 mm along either axis with a step size of 2.5 μm and a maximum resolution of 1/8 step, or 0.31 μm. It is controlled by an 8SMC1-USBhF microstep driver which communicates with a computer over USB.

REPRODUCIBILITY

The motorized positioner was mounted in the vertical position and tested using an increasing number of tungsten plates placed in different positions, as indicated in Figure 2. The behavior of the table was found to be independent of the location of the load.

To investigate the problems observed at the test beam, the 8MTF-102 was mounted vertically and an aluminum basket for tungsten plates was connected to the table at one of the four locations indicated in Figure 2.

The table was moved to the bottom of its range of motion, and moved upwards until it stalled. Increasing numbers of tungsten plates were added for each run. Each plate massed on average 0.87±0.01 kg. The highest position able to be reached for a load of a given mass is plotted in Figure 3. It is clear that the table loses its maximum range of motion well below the maximum specified load of 6 kg is reached.

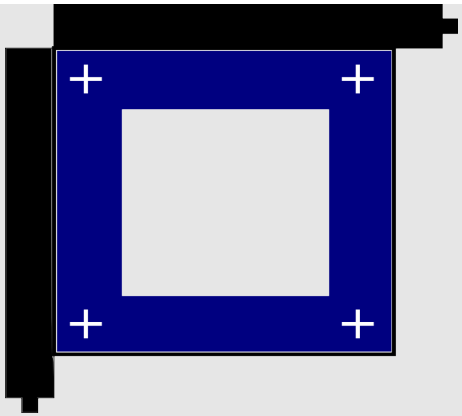

Figure 2: XY table schematic. The "+" marks indicate the four load positions. No dependence was found of table behavior on load position.

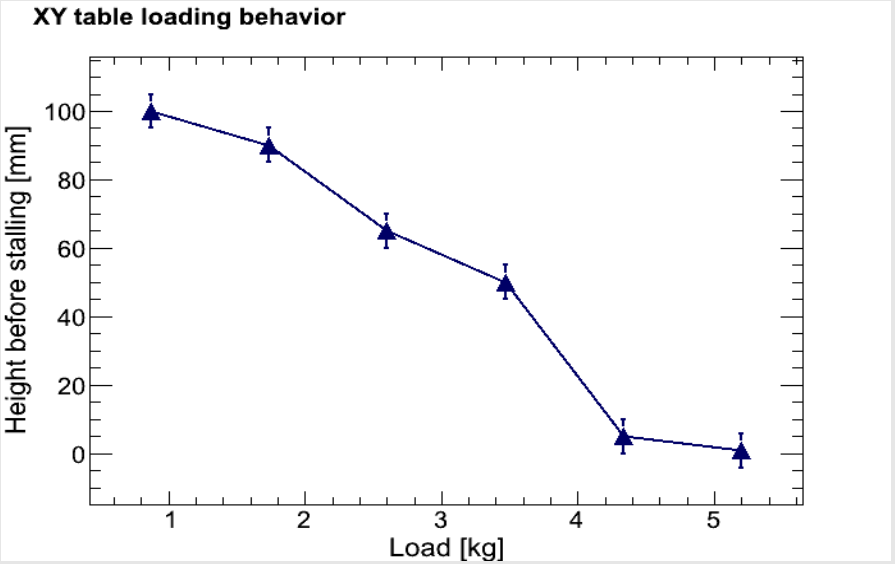

Figure 3: As the weight of the load increases (x-axis), the maximum height able to be reached by the table goes down to almost zero at 5 kg.

The major problem with this behavior is that the table does not know that it is stalled and continues to update its coordinates as if it were moving. This results in a loss of position information, and the coordinate system of the table must be reset using some known, reachable position.

TEMPORARY SOLUTION FOR TEST BEAM

In order to avoid this situation at the subsequent test beam, software limits were placed about 5 mm inside the usable range of the table given the load it was bearing. Also, a method to automatically and safely reset the coordinate system was implemented, in case of stalling.

CURRENT STATUS

The problem was unable to be resolved at AGH. The table is being sent to Standa for inspection and repair.

MC Simulation and Analysis

THE BHABHA SUPPRESSION EFFECT REVISITED

By

Strahinja LUKIĆ[1]

(1) Vinca Institute of Nuclear Sciences, Belgrade, Serbia

The calculations of the Bhabha Suppression Effect (BHSE) in luminosity measurement at the International Linear Collider (ILC) were revisited. Preliminary estimates of the BHSE at the Compact Linear Collider (CLIC) were performed for the first time, as well. The regularities in the largest contribution to the BHSE, the Beamstrahlung, are used to find event selection algorithms that minimize the BHSE at ILC, or reduce the sensitivity of the BHSE on the variations in the beam parameters. At CLIC, the BHSE is much larger, so that the precision of the luminosity measurements critically depends on the precise estimate of the BHSE.

Keywords: linear colliders, luminosity measurement, Bhabha scattering, Beam-beam effects, BHSE, numerical simulations

INTRODUCTION

Precise integral luminosity measurement at ILC will be performed by counting the Bhabha events recorded in the LumiCal detector in the Forward Region. The BHSE induced by the Beamstrahlung before the Bhabha scattering and by the electromagnetic deflection after the scattering represents an important source of systematic uncertainty in this context. As shown by C. Rimbault et al. [1] using the BHLUMI Bhabha event generator [2], together with a modified version of the Guinea-PIG software [3], the BHSE can be reduced by modification of the selection criteria for counting the Bhabha events in LumiCal.

In this work, this study was revisited to exploit the rather regular characteristics of the shift in the polar-angles of the outgoing electron-positron pairs after the Bhabha scattering.

Similar as in ref. [2], a set of 500,000 Bhabha events were produced with the energy in the center of mass (CM) frame = 500 GeV using the BHLUMI 4.04 software [3]. These events were then fed to the Guinea-PIG to simulate the Beamstrahlung and the Electromagnetic deflection effects.

POLAR ANGLES OF THE OUTGOING BHABHA PAIRS

As already shown in refs. [2] and [4], at ILC energies, the Beamstrahlung effect can be very well described using the assumption that approximately all radiation emitted by an electron-positron pair prior to the Bhabha scattering is emitted in the same direction along the beam axis. Thus the CM frame of the collision has non-negligible velocity directed, to a good approximation, along the beam axis. As a result, the polar angles of the outgoing particles, which are almost perfectly collinear in the CM frame, are shifted in opposite directions in the laboratory frame. The correlation between the shifts of the two polar angles is shown in

Fig. 1.

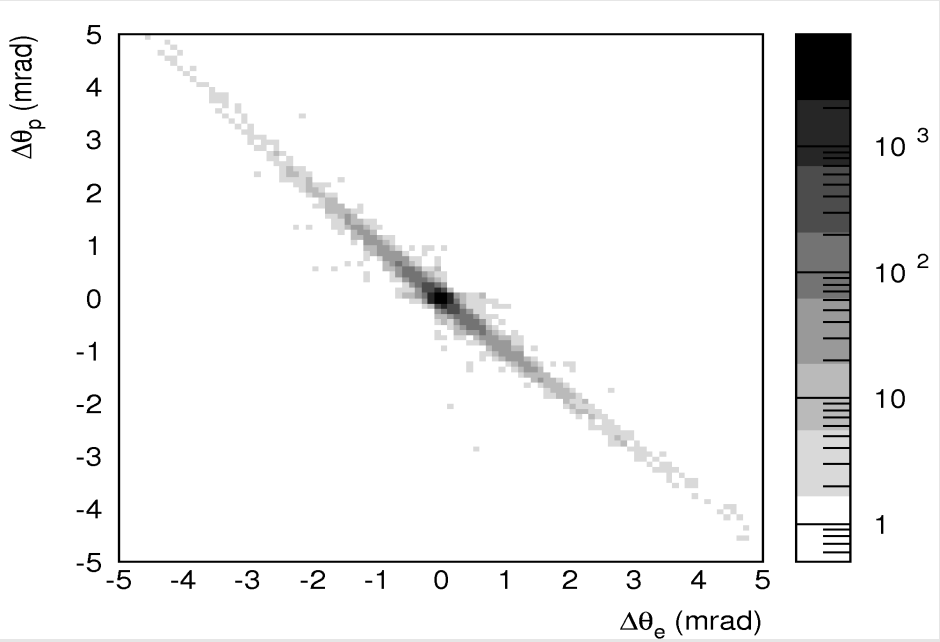

Figure 1: Correlation between the polar-angle shifts of the outgoing electron and positron in Bhabha scattering under influence of the Beamstrahlung effect

Because of that, the regions of the combined phase space of the two outgoing particles that are the most strongly affected by the BHSE are those where both polar angles are either in the immediate vicinity of the minimum angle θ_{min} or in the immediate vicinity of the maximum angle θ_{max} of the fiducial volume of the LumiCal (see Fig. 2).

BHSE REDUCTION AT ILC

Fig. 2 represents the 2D histogram plot of the polar angles of the outgoing Bhabha positrons versus the electrons. Selection cuts to the fiducial volume were applied before including the Beamstrahlung effect. The angular region enclosed by the thin box from 41 to 67 mrad in both θ_e and θ_p corresponds to the fiducial volume of the detector. The events appearing outside the fiducial volume represent the BHSE. The two small thick boxes enclose the areas the most strongly affected by the BHSE.

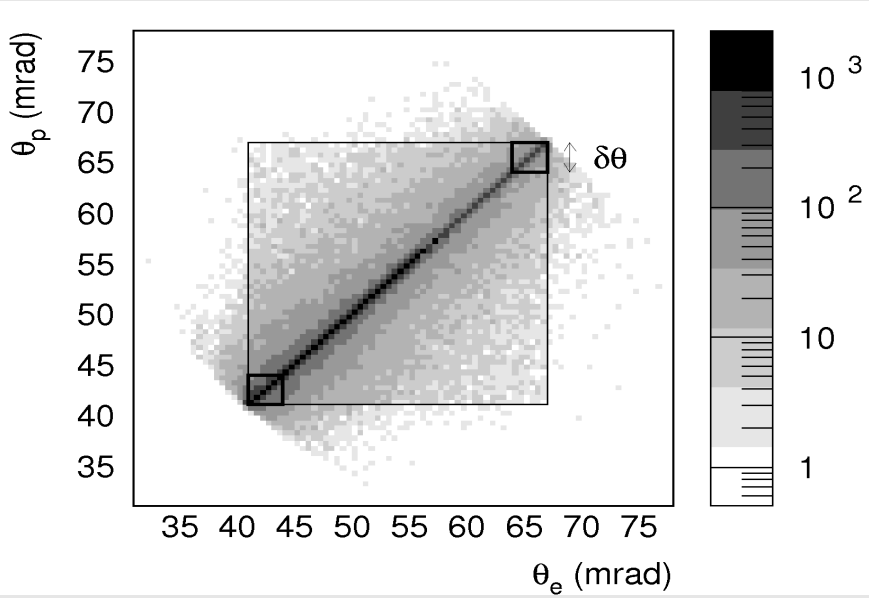

Figure 2: 2D histogram plot of the polar angles of the outgoing Bhabha positrons versus the electrons. Selection cuts to the fiducial volume were applied before including the Beamstrahlung effect. The two thick boxes represent the areas the most affected by the BHSE.

The BHSE at ILC can be effectively reduced if the regions within $\delta\theta$ from θ_{min} and θ_{max}, respectively, are excluded from the selection cuts.. Depending on $\delta\theta$, the BHSE at ILC can be reduced

to zero, or even made insensitive to variations in the horizontal bunch size σ_x (Fig. 3). Assuming ILD geometry and 500 GeV CM energy, for $\delta\theta$ = 2.8 mrad, the result of the simulation is BHSE = (0.01±0.06) %. The reduction of the BHSE comes at a moderate cost in efficiency. With $\delta\theta$ = 2.8, 31% of all Bhabha events hitting the geometrical volume of the LumiCal are counted towards the luminosity measurement. Compared to that, the number of counts in the entire fiducial volume represents 37% of all events hitting the geometrical volume. Thus a relative loss of statistic of 16% is induced by the modification of the selection criteria in order to suppress the BHSE. The region of low sensitivity to σ_x is situated around $\delta\theta$ = 4.8, which induces a relative loss of statistic of about 31%. In either case, the relative loss of statistic is not critical, since the relative statistical error of the luminosity measurement when the entire fiducial volume is used is of the order of 0.5×10^{-4} [5] on the yearly level.

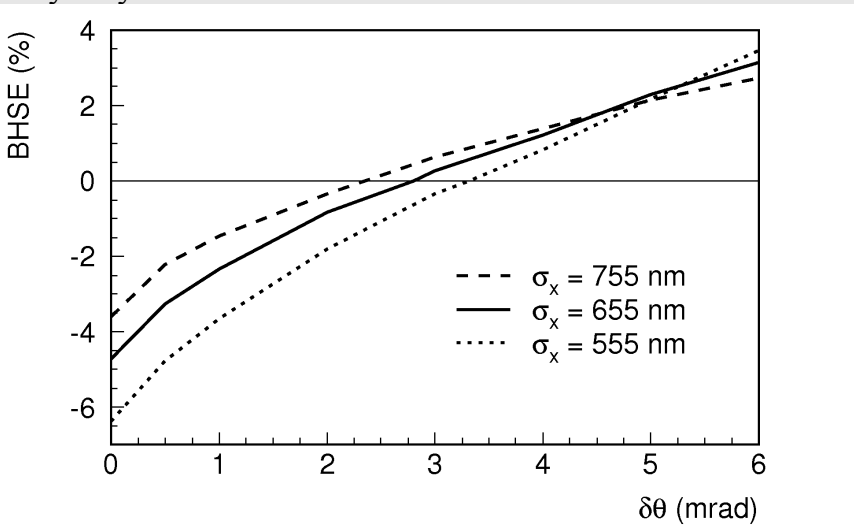

Figure 3: BHSE as a function of δθ for different horizontal bunch sizes σ_x

At 1 TeV in CM, for $\delta\theta$ = 3.5 mrad, the result is BHSE = (0.07±0.07) %, with a relative loss of statistic of 21%.

BHSE AT CLIC

Due to the intense Beamstrahlung at 3 TeV under the CLIC beam conditions, the BHSE at CLIC is estimated to around 70 %.

Fig. 4 represents a plot of the polar angles of the outgoing electron and positron from the Bhabha scattering at CLIC. The dashed lines represent the points that are directly reached by the Lorentz boost of the points (θ_{min}, θ_{min}) and (θ_{max}, θ_{max}) from the CM frame to the laboratory frame, under assumption that the CM moves along the beam axis. The edges of the distribution lie very close to these lines, indicating that the Beamstrahlung is the dominant effect, and that it is indeed predominantly emitted along the beam axis. The existing small spread of the distribution beyond the dashed lines is due to the electromagnetic deflection after the Bhabha scattering, as well as to the small transversal components of the Beamstrahlung momenta.

Such high BHSE cannot be meaningfully reduced with the selection criteria shown in the previous section. The precision of the luminosity measurement at CLIC thus critically depends on the possibility to precisely simulate and estimate the beam-beam effects. A method of data-driven control of the BHSE is necessary for that. A set of measurable parameters of the distribution needs to be defined that can be cross-checked between the simulation and the measured data. This is the topic of the ongoing work.

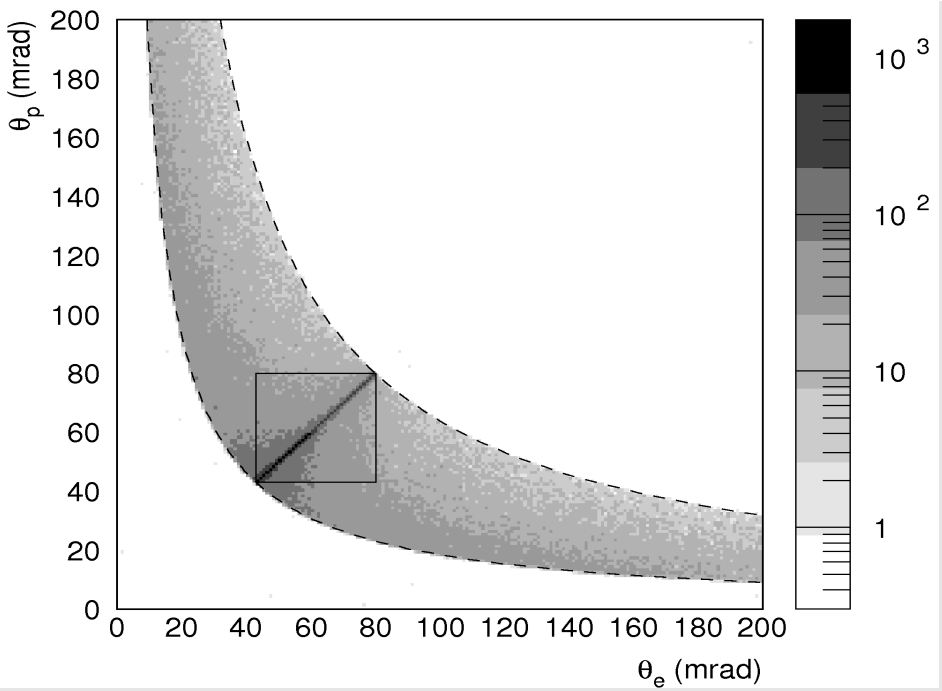

Figure 4: Histogram of the polar angles of the outgoing electron and positron from the Bhabha scattering at CLIC. The rectangular frame from 43 to 80 mrad represents the fiducial volume of the LumiCal.

CONCLUSIONS

It was shown that the regular nature of the polar-angle shifts induced by the beam-beam effects at ILC can be used to reduce the BHSE to zero, or to make it insensitive to the horizontal bunch size. Additional studies are necessary in order to propose optimal selection cuts that minimize the overall systematic effects, taking into account imperfections and uncertainties in the bunch shape parameters at the interaction point, the possible misalignment of the beams, uncertainties in the estimate of the BHSE, as well as the physics background.

Preliminary estimates of BHSE at CLIC were performed for the first time. At CLIC, the BHSE is much larger than at ILC, so that the precision of the luminosity measurement critically depends on the precise estimate of the BHSE. Data-driven methods of BHSE correction are necessary for this purpose. This will be the topic of the ongoing work.

REFERENCES

[1] C. Rimbault et al., *Impact of beam-beam effects on precision luminosity measurements at the ILC*, Journal of Instrumentation 2 (2007) P09001

[2] S.~Jadach et al., *Upgrade of the Monte Carlo program BHLUMI for Bhabha scattering at low angles to version 4.04*, Computer Physics Communications 102 (1997) 229 - 251.

[3] D.~Schulte, *Study of electromagnetic and hadronic background in the interaction region of the TESLA collider*, Ph.D. thesis, University of Hamburg (1996)

[4] K. Mönig, *Measurement of the Differential Luminosity using Bhabha events in the Forward –Tracking region at TESLA*, LC-PHSM-2000-60-TESLA (2000)

[5] H. Abramovicz et al., *Forward Instrumentation for ILC Detectors*, Journal of Instrumentation 5 (2010) P12002

PHYSICS BACKGROUND IN LUMINOSITY MEASUREMENT AT 1TEV AT ILC

By

Mila PANDUROVIĆ[1] AND Ivanka BOŽOVIĆ-JELISAVČIĆ[1]

(1) Vinca Institute of Nuclear Sciences, Belgrade, Serbia

In this paper we present the results of the investigation of the influence of two-photon processes on luminosity measurement at future linear collider ILC at center-of-mass energy of 1 TeV. The overall choice of selection criteria for the luminosity measurement with the respect to leading sources of systematic error is discussed. The potential of individual selection criteria to suppress physics background is discussed and comparison with the 500 GeV case is presented.

Key words: ILC, luminosity measurement, two-photon background

INTRODUCTION

The measurement of luminosity at ILC will proceed by using standard candle process: Bhabha scattering. Luminosity will be determined from the measurement of the event rate of Bhabha scattering in the luminosity calorimeter (LumiCal), which is located in the very forward region of the ILC. At ILC, a possibility of an upgrade to 1 TeV center-of-mass energy is foreseen. Since the measurement of integral luminosity at 500GeV is discussed in detail in [1] and [2], here we present possible event selections leading to the required physics background suppression in luminosity measurement at 1 TeV center-of-mass energy . In comparison to the 500 GeV case, the Bhabha scattering cross-section scales as 1/s, still being of order of a nb. Efects from the beam-beam interaction can be compensated by the proper choice of the detector 'counting region' as shown in [3]. Four-fermion processes, representing the main source of possible miscounts, are reviewed in the light of that newly proposed selection.

METHOD

Integrated luminosity at ILC will be determined from the total number of Bhabha events N_{th} produced in the acceptance region of the luminosity calorimeter and the corresponding theoretical cross-section σ_B.

$$L_{int} = \frac{N_{bha}}{\sigma_{bha}} \qquad (1)$$

The number of counted Bhabha events N_{exp} has to be corrected for the number of background events misidentified as Bhabhas, N_{bck}, and for the selection efficiency ε.

$$L_{int} = \frac{N_{exp} - N_{bck}}{\varepsilon \cdot \sigma_B} \qquad (2)$$

Luminosity calorimeter has been designed for the precise

determination of the total luminosity. This is compact electromagnetic sandwich calorimeter consisting of 30 longitudinal layers of silicon sensor followed by tungsten absorber and the interconnection structure. In the ILD concept assumed here [4], it is located at *z= 2573 mm* from the IP, covering the polar angle range between *31*and *78* mrad. It corresponds to the inner radius of the LumiCal of r_{min}*=80 mm*, and outer radius of r_{max}*=195 mm*.

Bhabha events, with cross-section of σ_{bha}*=(1.197±0.005) nb,* are simulated with BHLUMI [5] event generator, implemented in BARBIE V5.0 [6], a GEANT3 [7] based detector simulation of LumiCal.

Four-fermion NC processes $e^-e^+ \to e^-e^+ f\bar{f}$ are characterized by the large cross-section scaling with $\ln^2(s)$ and the typical topology where electron spectators are emitted at small polar angles carrying the most of the beam energy and thus can be miscounted as the Bhabha signal. In Figure 1, polar angle distribution of particles from four-fermion processes with energy greater than 60% of the beam energy, at the center-of-mass energy of 500 GeV and 1TeV, are given.

As can be seen from the Figure 1 the polar angle distribution of high energetic particles becomes steeper with the rise of the center-of-mass energy, meaning that these particles (primary electrons) would be emitted at at smaller polar angles than the LumiCal. This change in event topology will compensate the rise of the cross-section of these processes with the center-of-mass-energy.

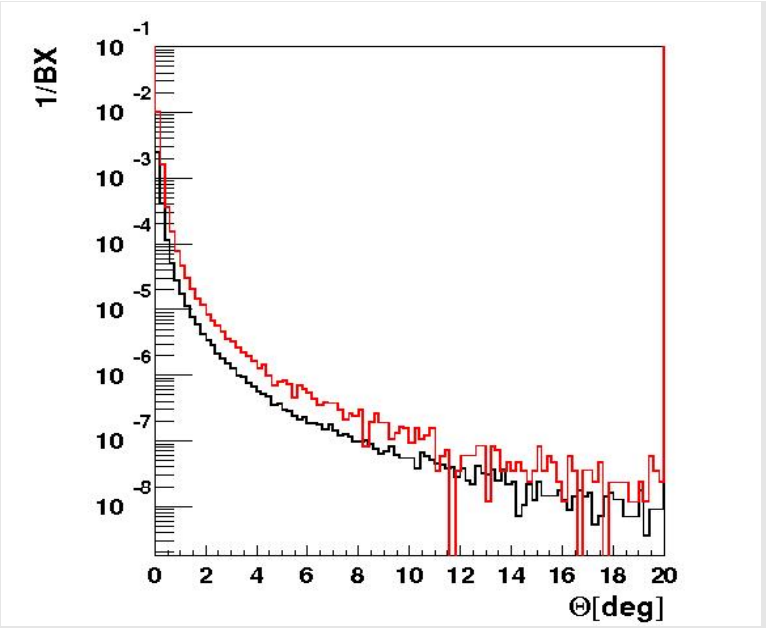

Figure 1. Polar angle distributions of final state particles with E>0.6E_{beam} from four-fermion processes, at the center-of-mass energy of 500 GeV (red) and 1 TeV(black).

In this study, fourfermion processes are simulated using WHIZARD V1.2 event generator [8]. 10^6 leptonic and $2\cdot10^5$ hadronic events are simulated including contribution of all neutral tree-level processes in the angular range [0.05,179.95] deg and at centre-of-mass energy of 1TeV. Total cross-section σ_{tot}*=(0.78±0.05) nb* is obtained, with following assumption on event generation:

- invariant masses of the outgoing lepton pairs are greater than *1 GeV/c^2*

• momentum transferred in photon exchange is greater than 10^{-4} *GeV/c.*

EVENT SELECTION

Two electromagnetic clusters carrying the full beam energy, originating from collinear and coplanar Bhabha particles, identify signal events. Based on these topologicalcharacteristics of the signal several selection criteria can be employed :

- relative energy, defined as a fraction of beam energy, Ebeam, carried by the Bhabha particle (EL,ER stands for the particle energy deposited at the left and right side of the LumiCal):

$$E_{rel} = \frac{E_L + E_R}{2 \cdot E_{beam}} \qquad (3)$$

- energy balance:

$$E_{bal} = |E_L - E_R| \qquad (4)$$

- colinearity and coplanarity, defined as the difference in polar (azimuthal) angles of Bhabha particles:

$$\Delta\theta = |\theta_L - \theta_R| \qquad \Delta\varphi = |\varphi_L - \varphi_R| \qquad (5,6)$$

Colinearity of Bhabha events is to small extent distorted due to the beam-beam interaction effect [9]. This leads to the effective reduction of the Bhabha cross-section in the detector fiducial volume (BHSE). It has been shown [9],[3] that the effect is more pronounced with rise of the center-of-mass energy. Beam-beam interaction is accommodated by using: asymmetric cuts on particle polar angle as proposed for the 500 GeV case in [9], or by the proper choice of the detector counting volume that downscales the BHSE effectively to zero [3] . In the later case the regions within $\delta\theta$ squares are excluded (Figure 2 [3]) . For $\sqrt{s}$ = 1TeV, $\delta\theta$ is found to be 3.6 mrad [3].

Effects of various combinations of the selection criteria on the background to signal ratio are given in the Table 1, assuming the center-of-mass energy of 1TeV. In the same table, the comparison with the 500GeV [1] case is presented. Relative statistical error of B/S estimation is also given.

Table 1. Physics background to signal ratio given at the center-of-mass energy of 1Tev and 500 GeV, for different event selections.

Selection criteria	***B/S* 1TEV**	**Δ(B/S) [%]**	***B/S* 500 GeV**
$[\theta_{min}$+4mrad, θ_{max}-7mrad]; E_{rel}	$1.4\cdot10^{-3}$	±19.5	$3.7\cdot10^{-3}$
$[\theta_{min}$+4mrad, θ_{max}-7mrad]; E_{rel}; $\|\Delta\varphi\|<5^o$	$1.1\cdot10^{-3}$	±30.0	$2.9\cdot10^{-3}$
$[\theta_{min}$+4mrad, θ_{max}-7mrad]; E_{bal}; $\|\Delta\varphi\|<5^o$	$1.0\cdot10^{-3}$	±44.9	$2.2\cdot10^{-3}$
$\|\delta\theta\|<0.06^o$; E_{rel}; $\|\Delta\varphi\|<5^o$	$0.9\cdot10^{-3}$	±29.3	$2.6\cdot10^{-3}$
$\|\delta\theta\|<0.06^o$; E_{bal}; $\|\Delta\varphi\|<5^o$	$0.8\cdot10^{-3}$	±37.6	$1.6\cdot10^{-3}$
E_{rel}; Exclusion region ($\delta\theta$=3.6 mrad)	$1.3\cdot10^{-3}$	±29.4	\

Also, for the reason of completnes two-photon systems of beamstrahlung photons taking part into $e^+e^-\gamma\gamma \rightarrow X$ processes are are simulated with the GUINEAPIG generator [10] and analyzed before hadronization in the full polar angle range. Acquiring only that total energy of the system is 80% of the $\sqrt{s}$, with no angular criteria applied, the upper limit from this source of background in the LumiCal is estimated to be less than $2 \cdot 10^{-3}$ with respect to the signal.

CONCLUSION

The rise of the cross-section of two-photon processes with the center-of-mass energy, posses no fundamental restriction on the precision of the luminosity measurement. This is mainly due to the change in topology of the primary electron-positron pair being emitted at lower polar angles bellow the LumiCal. For all the selection discussed, physics background can be in suppressed to the permille level with respect to the signal. In particular, the selection that effectively reduces BHSE to zero does not compromise the suppression of physics background.

REFERENCES

[1] M. Pandurović, "Background in luminosity measurement at ILC and improvement of b quark identification at H1 using multivariate approach", PhD thesis, Univerisity of Belgrade, 2011.

[2] W. Lohman, I. Bozovic-Jelisavcic, M. Pandurovic, I. Smiljanic, T.Jovin et al., "Forward instrumentation for ILC detectors", *JINST* **5** P12002 , 2010.

[3] S. Lukić, "The Bhabha suppression effect at ILC revisited", these proceedings.

[4] T. Behnke et al., ILD working group, "Letter of Intent", ILD web site, http://www.ilcild.org/documents/ild-letter-of-intent .

[5] Jadach S., Placzek W., Richter-Was E., Ward B.F.L. and Was Z., BHLUMI, A Monte Carlo Event Generator for BhaBha Scattering at Small Angles, Version 4.04.

[6] Pavlik B., BARBIE V5.0, Simulation package of the TESLA luminosity calorimeter, available from Bogdan.Pawlik@ifj.edu.pl

[7] Application Software Group, 1994. Computing and Networks Division GEANT—Detector Description and Simulation Tool, CERN Program Library Long Writeup W5013 , CERN, Geneva, Switzerland, http://wwwasdoc.web.cern.ch/wwwasdoc/geant_html3/geantall.html

[8] Kilian W., Ohl T., Reuter J., WHIZARD: Simulating Multi-Particle Processes at LHC and ILC , arXiv: 0708.4233 http://arxiv.org/abs/0708.423.3

[9] Rimbault C., Bambade P., Mönig K. and Schulte D., Impact of beam-beam effects on precision luminosity measurements at the ILC, 2007 JINST 2 P09001 doi: 10.1088/1748-0221/2/09/P09001.

[10] D. Schulte, Ph.D. Thesis, University of Hamburg 1996, TESLA-97-08.

BEAMCAL RECONSTRUCTION SOFTWARE

By

Aura ROSCA

DESY, Hamburg, Germany

The reconstruction of the energy of isolated electrons in the beam calorimeter of the ILC detectors is described. Using an appropriate subtraction of the pair background and a shower clustering algorithm taking into account the longitudinal shower profile, the deposition of the high energy electron can be detected with high efficiency. The electron energy is deduced from the cluster energy measurement. The electron direction is assumed from the interaction point towards the cluster.

Key words: beamstrahlung, high energy electron, sensor pad, cluster

1. INTRODUCTION

A strategy for the reconstruction of electrons in the beam calorimeter of the ILC detectors is presented in this paper. Electron identification in the very forward region will be important in several physics analyses, including new particle searches. Electron reconstruction in Beamcal can only use information from this detector, since the forward tracking detectors cover the polar angle region down to 100 mrad. A brief description of the BeamCal detector is given in Section 2.

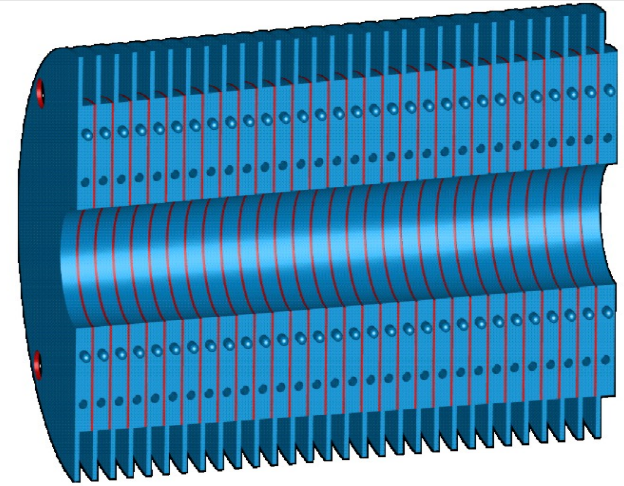

Figure 1. Sketch of the structure of a half barrel of the sandwich beam calorimeter. For the study presented here the outer radius is 15 cm , equal to the length along the beam-pipe. Sensors are interspersed between tungsten disks. The thickness of the absorber disks is one radiation length and of the sensors 0.5 mm.

A large amount of low energy electron - positron pairs originating from beamstrahlung will deposit their energy in Beamcal. Such beamstrahlung pairs deflected in the beam calorimeter will provide important information for beam diagnostics, but the price to be paid is that the high energy electrons from physics processes will have to be reconstructed on top of the

pair background depositions. Therefore the reconstruction algorithm uses in a first step a procedure for background subtraction. The background subtraction technique is described in Sect. 3, while the electron clustering applied in the next step of the reconstruction algorithm is described in Sect. 4. Finally, the implementation of the algorithm in the common reconstruction framework of the ILD detector is presented in Sect. 5.

2. THE BEAMCAL

Two electromagnetic calorimeters are foreseen in the very forward region of the ILC detectors at the interaction point, LumiCal for a precise measurement of the luminosity and BeamCal for a fast estimate of the luminosity and control of the beam parameters. In the same time they will both improve the hermeticity of the detectors. BeamCal will cover a polar angle region between 5 and 40 mrad and LumiCal between 31 and 77 mrad. A third electromagnetic calorimeter, GamCal, will be placed about 100 m downstream of the detector to assist in beam tuning. A pair monitor, consisting of a layer of pixel sensors will be positioned just in front of BeamCal to measure the distribution of beamstrahlung pairs and give additional information for beam parameter determination. Finally, LHCAL will be a hadron calorimeter that will extend the coverage of the HCAL endcap to smaller polar angles. In the following only some of the relevant characteristics of the BeamCal used for electron reconstruction are presented. A detailed description of the very forward region of the ILC detectors can be found in reference [1].

The BeamCal is designed as a sandwich calorimeter with a structure as shown on Figure 1, where a half barrel of the calorimeter is depicted. It contains 30 layers of tungsten absorber disks with a thickness of one radiation length and thin sensor layers with a thickness of 0.5 mm. The sensor layers are subdivided into pads which, for the study described below, have a size of about 8 mm. Fine granularity is necessary in order to identify the localized depositions from high energy electrons and photons on top of the wider spread depositions from low energy electron – positron pairs that originated from beamstrahlung. These latter depositions are useful for a bunch-by-bunch luminosity estimate and the determination of the beam parameters [2]. The other important role of the Beamcal is the identification of high energy electrons and photons at small polar angles. This is important in order to veto two-photon processes that are very large backgrounds to new particle searches as for instance, super-symmetric particles. In the following I will concentrate on the algorithm developed for the single electron reconstruction.

3. SUBTRACTION PROCEDURE

The difficulty related to the background subtraction comes from the fact that the background fluctuates from one bunch crossing to the next. This is illustrated on Figure 2 where the depositions on the same pad from about 2000 BX simulated with GuineaPig [3], for nominal beam parameters are shown.

Such distributions were obtained for each sensor pad of the detector, this way a background map was constructed to keep the information of the average and root-mean-square values of the background depositions in all the pads of BeamCal. Now it is

possible to subtract the value of the average background energy from the sum of the background and signal depositions on each pad, or equivalently, add the background fluctuations to the signal depositions and obtain a smeared energy distribution for the signal. This latter procedure we implemented in Marlin. We generate Gaussian background fluctuations with mean zero and the root-mean-square read from the map for each pad, randomly picking up a value from the distribution and add it to the corresponding signal energy deposition in the same pad. Thereafter we apply the shower search algorithm described briefly in the following section.

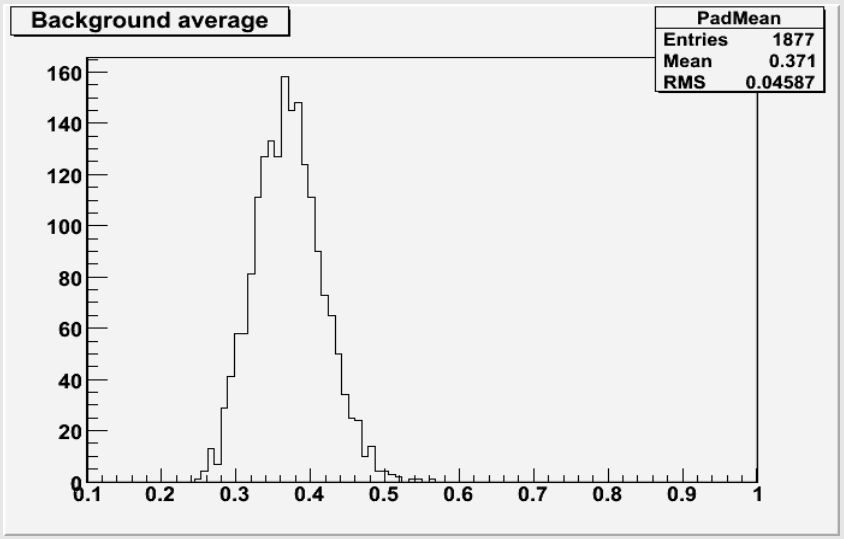

Figure 2. Background depositions in one pad of the Beamcal from about 2000 bunch crossings.

4. ELECTRON CLUSTERING

The electromagnetic showers initiated by electrons (or photons) deposit their energy in several pads of the BeamCal. For a single electron (or photon) reaching the beam calorimeter, most of the energy is collected in a small number of sensors. Electrons with the energy of 250 GeV impinging at the center of a pad for instance deposit about 97% of their incident energy in a 3 x 3 pad window.

A detailed description of the clustering algorithm can be found elsewhere [4]. Here only the main steps of the algorithm are presented.

The shower search is done from the 5th to the 30th layer, to exploit the longitudinal shape of the signal showers. If a chain of 10 consecutive pads within this range is found, then a tower is defined. The adjacent towers around the center tower with the maximum energy are considered and a cluster is defined. Finally, the sums of depositions on the pads in the clusters which are higher than one root-mean-square of the background deposition in the same pad are used to determine the energy and position of the cluster. Further the electromagnetic clusters are assumed to be neutral and assigned a particle rest mass of zero. The cluster energy combined with this mass assignment is used to define the particle 4-momentum vector. The simple clustering scheme used here assumes that the momentum of the electron (or photon) reconstructed from a cluster points from the event interaction point towards the cluster. This is however correct only for the photon, since the electron trajectories are curved by the solenoidal magnetic field.

5. IMPLEMENTATION IN MARLIN

The reconstruction algorithm has been implemented into the Marlin framework [5]. Fig. 3 shows the algorithm as a flow chart. The response of the beam calorimeter to single electrons was simulated with Mokka [4] and the detector model ILD_00fw. The BeamCal collection of hits is used and the signal energy deposition on each pad is obtained. The background map is read and the signal depositions are smeared accordingly. Then the shower reconstruction algorithm is applied and finally the relevant collections of reconstructed clusters and particles are filled and added to the event.

A new Marlin processor was written in C++ to do the tasks described before. A dynamic array is used to keep the information for each pad that is input to the shower search algorithm which was re-written as a C++ class. This processor was included in MarlinReco in the newest release of the ILCSoft version 01-12. The class contains methods to do all the tasks that were done in the past by separate pieces of code. GetReconstrCoordinates is the interface method that provides the reconstructed quantities, as for instance the cluster energy, the cluster Cartesian coordinates, and also a local position in the beam calorimeter in terms of the ring and pad where the cluster has been reconstructed.

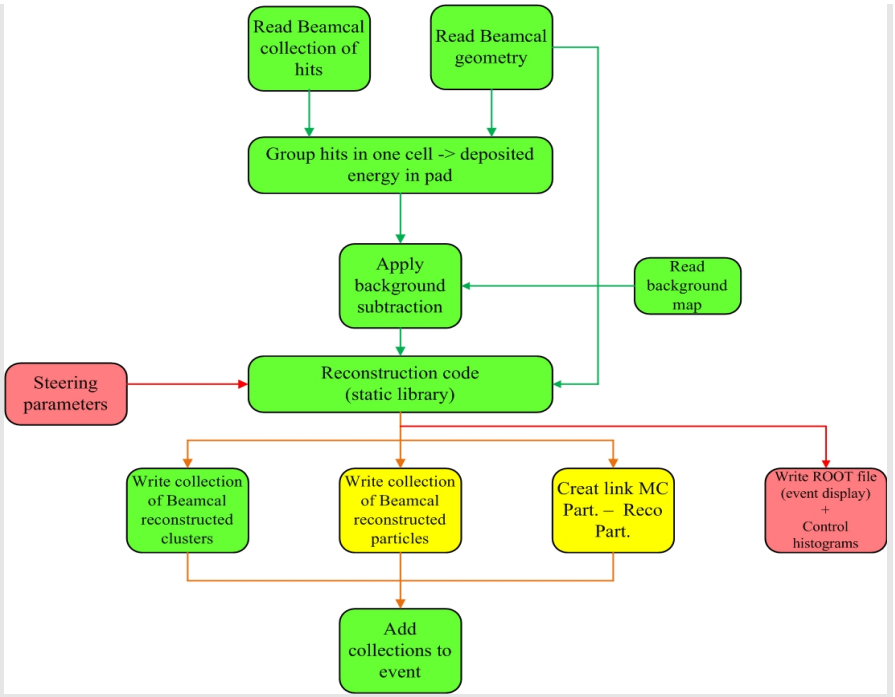

Figure 3. The electron reconstruction algorithm in the beam calorimeter is shown as a flow chart.

6. CONCLUSIONS

A strategy for the reconstruction of electrons on top of the pair background in the beam calorimeter of the ILC detectors has been presented. It uses an appropriate subtraction procedure of the background and a clustering algorithm that takes into account the longitudinal profile of the showers produced by high energy electrons. Next the algorithm will have to be optimized for high efficiency and low fake rate [6].

REFERENCES

[1] H. Abramowicz et al., Forward instrumentation for ILC detectors, JINST 5 P12002 (2010).

[2] Ch. Grah, A. Sapronov, Fast Luminosity Measurement and Beam Parameter Determination, EUROTeV-Report-2007-006 (2007).

[3] O. Novgorodova, Studies on the electron reconstruction efficiency for the beam calorimeter of an ILC detector, physics.ins-det/1006.3402v1.

[4] Guinea-Pig:https://trac.lal.in2p3.fr/GuinePig/wiki.

[5] ILC simulation and reconstruction software: http://ilcsoft.desy.de/portal.

[6] A. Rosca, Electron reconstruction in the beam calorimeter, Proceedings of the International Workshop on Future Linear Colliders, Granada, Spain, September 2011, in preparation.

Forward Region at CLIC

UPDATE ON THE MECHANICAL INFRASTRUCTURE FOR VERY FORWARD CALORIMETER BEAM TESTS

By

Christophe BAULT, Eric DAVID, Konrad ELSENER, Francois-Xavier NUIRY, Adrien VARLEZ

CERN, Geneva, Switzerland

In the framework of the AIDA collaboration, a mechanical infrastructure for future particle-beam tests of forward calorimeter sensors is under construction at CERN. The device will allow installing up to 30 tungsten plates interleaved with sensors. The high mechanical accuracy required for LumiCal is matched by the design of the device. Flexibility to allow for both LumiCal and BeamCal sensor tests with different front-end electronics is built into the design. This paper provides an updated version of the design, allowing the use of the device with existing sensor and read-out boards.

Keywords - tungsten, sensor, mechanics, precision

INTRODUCTION

The FCAL collaboration [1] is participating in AIDA [2], a recent infrastructure project funded partly by the European Union. In this context, it is proposed to build a flexible mechanical infrastructure allowing the test of individual sensors or complete segments of the LumiCal or BeamCal calorimeters.

The CERN PH-DT group (detector technology group of the physics department) has been mandated to design and build this mechanical infrastructure based on a functional specification [3]. The device should allow inserting of up to 30 tungsten plates of 3.5 mm thickness paired with sensor planes. The distance between tungsten plates should be either 2, 1 or 0.5 mm. Given the typical LumiCal and BeamCal sensors under investigation, the size of the tungsten plates should be 14x14 cm^2. The challenge stems from the requirement of 50 micron mechanical accuracy (roughness, flatness) of each tungsten plate and of the distance between the plates.

In a first iteration, two design proposals have been worked out. These were presented to the FCAL collaboration at its meeting held from 30 May to 1 June 2011 in Predeal, Romania [4]. As a result of the discussions at that meeting, it was decided to give priority to further work on one of the proposals, although this would only allow a structure with distances between tungsten plates of either 2 or 1 mm. Most importantly, it turned out to be crucial to use the structure with the existing sensor boards (PCBs) and read-out boards – a modified version of these boards would not become available in the coming two years. This paper provides an update of the design of the mechanical infrastructure.

MODIFIED DESIGN PROPOSAL

The basic concept of the first design proposal of spring 2011 is to use a set of three precisely machined "combs", precision-mounted on a solid base frame (see Figure 1). All parts are made of stainless steel. The three precision-"combs" are equipped with brass springs. The two additional "combs", on the top of the frame, are not used for the alignment – they are flipped open to insert the tungsten plates and sensors.

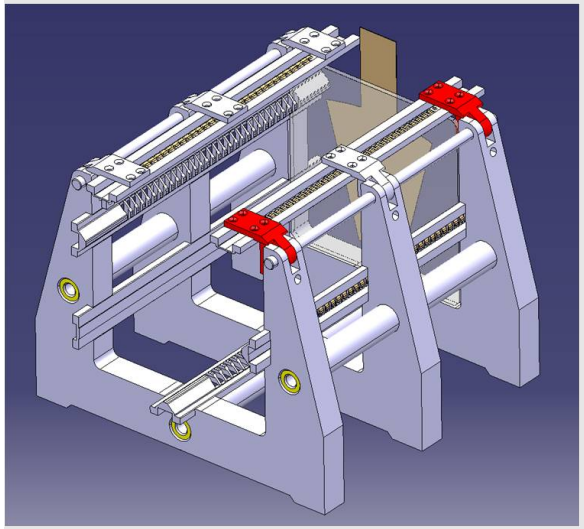

Figure 1. Isometric view of the mechanical infra-structure of the first design proposal [4].

Figure 2 shows the modified version of this design, considerably larger in order to accommodate the existing LumiCal sensor boards with an overall width of 21 cm.

In order to limit the expenditures for the tungsten plates, the concept of PermaGlass [5] frames was introduced in the new design. After discussion, it turns out that these frames help to considerably increase the flexibility for the use of the mechanical infrastructure under design: Different types of PermaGlass frames may be built, for tungsten plates, for existing or forthcoming LumiCal and BeamCal sensor boards, etc. As examples, the existing sensor board in its frame is shown in Figure 3, a tungsten plate inserted in its frame in Figure 4, while the tungsten plate assembled into the mechanical infrastructure is shown in Figure 5. Figure 6 shows a schematic view of a comb with two tungsten plates, with details of the dimensions for the case of a distance between tungsten plates of 2 mm.

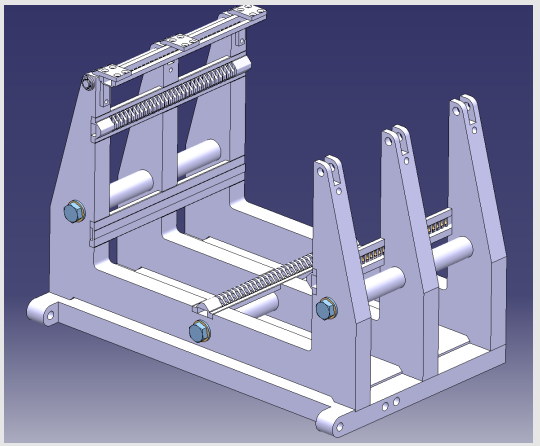

Figure 2. The modified wider version of the mechanical infrastructure, designed to accommodate-date the existing sensor board.

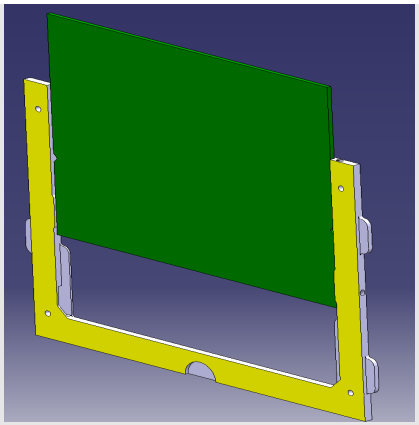

Figure 3. PermaGlass frame as holder for the existing LumiCal sensor board.

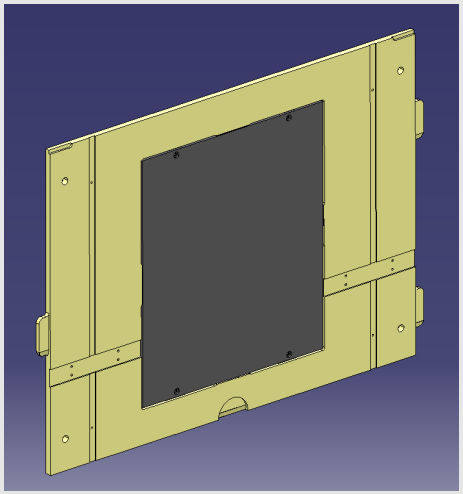

Figure 4. PermaGlass frame as casette for a tungsten plate.

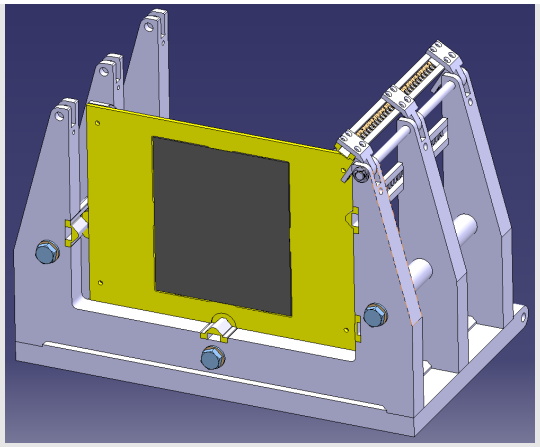

Figure 5. One tungsten plate in its PermaGlass holder, inserted into the mechanical infrastructure.

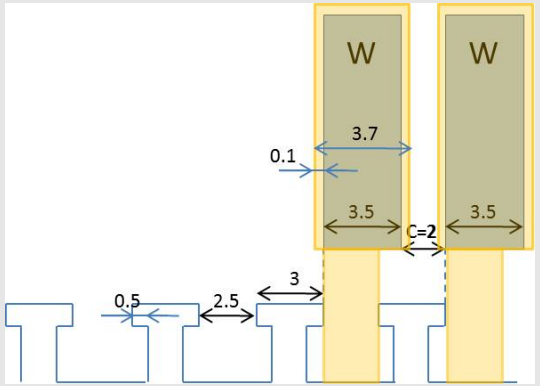

Figure 6. Schematic side view of the comb structure with two tungsten plates in their PermaGlass frames.

ROTATION OF STRUCTURE TO MEASURE COSMIC MUONS

While this mechanical infrastructure is primarily designed to work in test beams at accelerators, one of the requirements specified was to also be able to rotate the structure and use it to measure cosmic muons. A first proposal to accommodate this feature has been worked out, and is sketched in Figure 7.

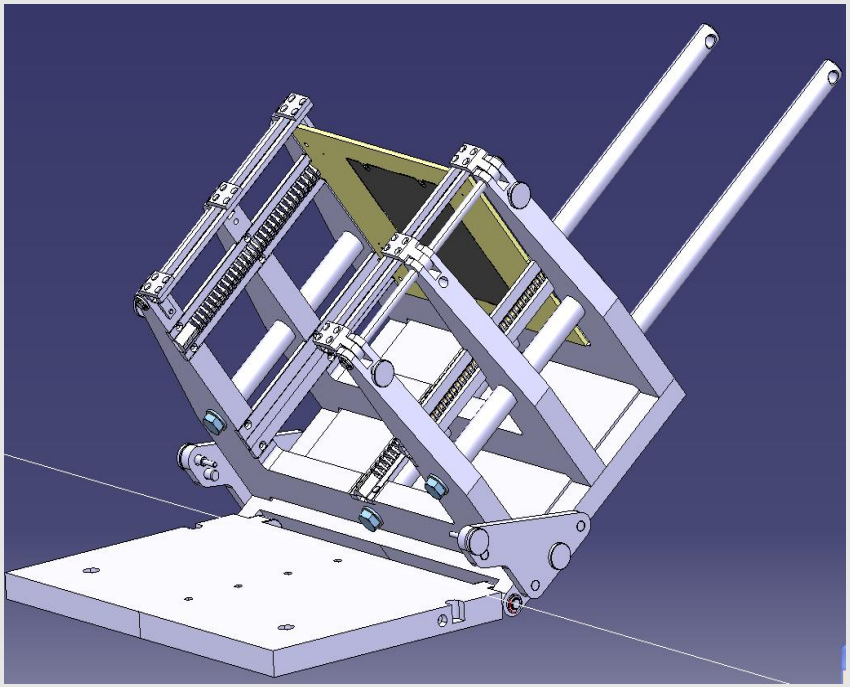

Figure 7. Proposed solution to allow the use of the mechanical infrastructure both for horizontal beams and cosmic (vertical) muons.

TUNGSTEN PLATES

During the design phase for this mechanical infrastructure, it became clear that the quality of the tungsten plates (roughness, flatness) is of prime importance if one wants to reach the goal of 50 μm accuracy on the distance between two adjacent tungsten plates. Contacts with industry are being pursued – most likely the material will be an alloy of tungsten with a few percent of other metals, which has proven to be more easily machined and handled than pure-tungsten plates.

PROTECTION AROUND THE STRUCTURE

In addition to the mechanical infrastructure itself, a light-tight protection (a box) around the device is part of this project. Moreover, it is requested that such a box acts, at the same time, as a Faraday cage to shield the sensors against electronics noise. The design of this box is in progress.

SUMMARY AND NEXT STEPS

During 2011, the detailed design proposal for this mechanical infrastructure has evolved at CERN, and reached maturity. Construction of the device is imminent. In parallel, the design of the protection “box” is approaching completion. It is expected that the mechanical infrastructure will be available for use in test beams in the course of 2012.

The procurement of the tungsten plates is the responsibility of several institutes within the FCAL collaboration. Contacts with industry are under way concerning in particular the availability of

tungsten plates with very good surface quality.

REFERENCES

[1] The FCAL collaboration, http://fcal.desy.de/

[2] Advanced European Infrastructures for Detectors at Accelerators (AIDA), http://aida.web.cern.ch/aida/index.html

[3] K. Elsener, **"**Mechanical Support Structure as part of an AIDA infrastructure for testing high-accuracy very forward calorimeters" (Functional Specification), https://edms.cern.ch/document/1116164/

[4] C. Bault et al., Proceedings of the XVII FCAL collaboration meeting, Predeal, Romania (2011), http://www.ifin.ro/fcal_2011/

[5] E.g. "PERMAGLAS ME", from Resarm SA, France

BACKGROUND IN THE CALORIMETER ENDCAPS

By

André SAILER[1,2]

(1) CERN, Geneva, Switzerland
(2) Humboldt-Universität zu Berlin, Berlin, Germany

Backgrounds from strong beam-beam interactions at linear colliders have to be studied in all sub-detectors. Here the simulation studies of the background of incoherent pairs and γγ → hadron events in the ECal and HCal endcaps and the estimated occupancies are presented. It is shown that these background sources deposit a significant amount of energy in both calorimeter endcaps, but a large impact on the occupancy can only be seen at small radii in the HCal endcap.

Key words Beam-beam Background, Calorimeters, CLIC, occupancy

INTRODUCTION TO CLIC

The Compact Linear Collider (CLIC) is designed for electron-positron collisions at c.m.s. energies up to 3 TeV [1]. The normal-conducting RF cavities operate at a gradient of 100 MV/m, and the RF power is distributed along the accelerator by a 2.4 GeV, high intensity `drive beam'. In order to achieve the desired luminosity, CLIC operates with bunch trains of 312~bunches separated by 0.5~ns, with a repetition rate of 50~Hz and transverse bunch size of 45 nm by 1nm and a length of 44 μm. A number of design considerations have led to a crossing angle at the interaction point of 20 mrad. The large number of electron-positron pairs produced by the beam-beam interaction has to be studied in a full detector simulation to evaluate and minimise the impact on the detector performance.

The detector is implemented in the GEANT4 [2] based detector simulation MOKKA [3], and the simulations are run with the QGSP_BERT_HP physics list and a range cut of 5 μm. More details of the forward region, the beam-induced background at CLIC and their impact on the tracking detectors can be found elsewhere [4]. In the following only the impact of the γγ → hadron and incoherent pair background on the calorimeter endcaps will be discussed. More details can be found in [5].

OCCUPANCIES IN THE CALORIMETER ENDCAPS

To estimate the occupancy from backgrounds in the calorimeters, some assumptions have to be made regarding the pad size and time resolution of the detectors. The pad sizes are fixed in the GEANT4 implementations of the detector models. The electromagnetic calorimeter (ECal) is a silicon–tungsten sandwich calorimeter with a 5.08×5.08 mm² pad size, and a silicon thickness of 0.5 mm. The hadronic calorimeter (HCal) endcap is a scintillator–steel sandwich calorimeter with 30×30 mm² pad size and 5 mm thick scintillators [6].

Each bunch train is 156 ns long, but the hadronic shower development has long tails in time, therefore the maximum

acceptance time of the sensors was increased to 300 ns after the first bunch crossing. The total readout window of 300 ns is divided into 12 windows of 25 ns each. The occupancy is quoted as hits in a given number of time windows with an energy deposit above the threshold of 40 keV in the ECal and 300 keV in the HCal. For example, an occupancy of 2.0 means that for the same pad two time windows received a significant energy deposit during the 300 ns related to a bunch train.

DEPOSITED ENERGY IN THE CALORIMETER ENDCAPS

Figure 1 shows the energy deposits from incoherent pairs and $\gamma\gamma \rightarrow$ hadrons in the ECal and HCal endcaps. All distributions except those linked to secondary particles from incoherent pairs in the HCal show the peak for minimum ionising particles (MIPs). The total reconstructed energy per train is 2 TeV in the ECal endcaps and 16 TeV in the HCal endcaps from secondaries of incoherent pairs and 11 TeV in the ECal endcaps and 6 TeV in the HCal endcaps from $\gamma\gamma \rightarrow$ hadron events.

OCCUPANCY IN THE ELECTROMAGNETIC CALORIMETER ENDCAP

The shower maximum for the particles from $\gamma\gamma \rightarrow$ hadrons is around the sixth ECal layer, while the even lower energy particles from the incoherent pairs have their maximum already in the first layer (Figure 2a). The increase in the number of hits for incoherent pairs from layer 23 to 29 is caused by particles scattering into the backside of the ECal. As expected from the number of hits per layer, the radial distribution averaged over the azimuthal angle shows that the background in the endcap of the ECal is dominated by particles from the $\gamma\gamma \rightarrow$ hadron interactions (Figure 2b). The highest occupancies are observed at small radii. The dip in the occupancy at R $\approx$ 0.25 m is caused by the beam pipe, which shadows a part of the ECal endcap.

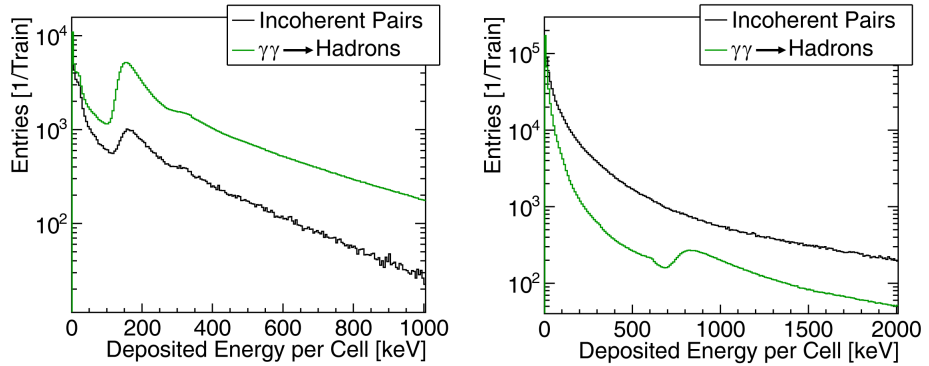

(a) (b)

Figure 1. Distribution of the energy deposit in all calorimeter pads for (a) the ECal endcap and (b) the HCal endcap from incoherent pairs and γγ → hadrons.

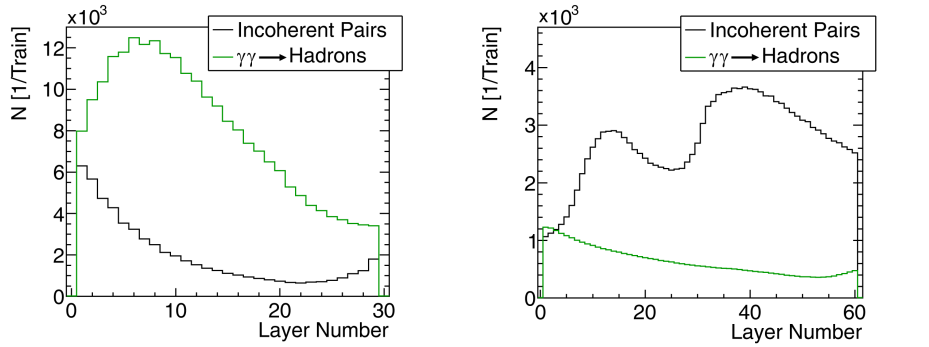

(a) (b)

Figure 2. (a) Number of time windows with energy deposits above threshold for the ECal Endcap from incoherent pairs and γγ → hadrons per layer. (b) The radial distribution of the train occupancy per pad, averaged over layers 5 to 10.

OCCUPANCY IN THE HADRONIC CALORIMETER ENDCAP

For the $\gamma\gamma \rightarrow$ hadron events the majority of energy deposits is caused by direct hits into the HCal endcap, and the number of energy deposits decreases with increasing layer number (Figure 3a), except for a slight increase in the last few layers. The source of this increase of the signal in the last few layers is still under investigation. The material following the HCal endcap is the Yoke Plug, made out of iron, like the HCal endcap absorber. It could be an effect due to the magnetic field, as this region is close to the end of the solenoid coil, and the magnetic field changes, because of the yoke as well. For products from the incoherent pairs, two broad peaks in the number of hits are visible. This distribution is due to the provenance of the particles. A large number of secondary particles is produced by the showers of the incoherent pairs in the BeamCal, which is located inside the HCal endcap between layers 20 and 40. As there is an additional iron 'BeamCal Support' around the BeamCal and thus better shielding of the HCal, there is a dip in the number of hits between layers 20 and 40. Most of the energy deposits from secondaries produced in the BeamCal are at the innermost radius (R = 0:4 m) of the HCal endcap.

In this region up to ten out of the twelve time windows see an energy deposit. Beyond a radius of 0.6 m the occupancy falls to about one energy deposit above threshold per train (see Figure 3b). At R = 1 m the occupancy from $\gamma\gamma \rightarrow$ hadron events is equal to that of incoherent pair secondaries, whose occupancy decreases more rapidly.

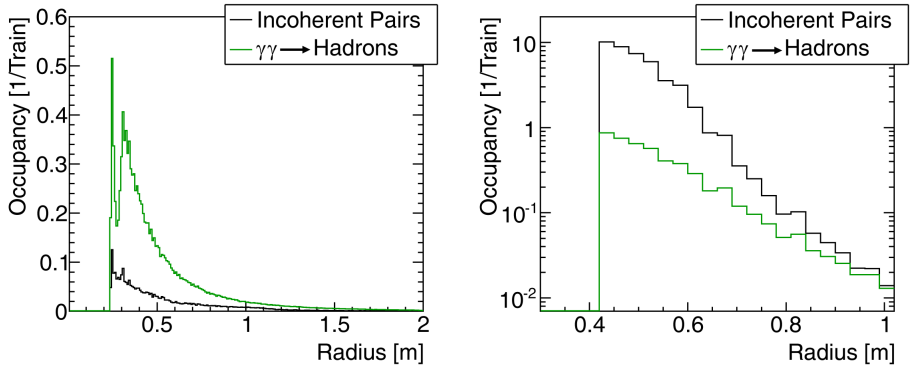

(a) (b)

Figure 3. (a)Number of time windows with energy deposits above threshold for the HCal Endcap from incoherent pairs and γγ →hadrons per layer. (b) The radial distribution of the train occupancy per pad, averaged over layers 35 to 45.

CONCLUSIONS

The occupancy in the ECal endcap is reasonable and dominated by the $\gamma\gamma \rightarrow$ hadron events. The occupancy in the HCal endcap at small radii is too large. However, due to the dominance of secondary neutrons produced in the BeamCal for causing the occupancy, a redesign of the support tube inside the calorimeter endcap, or finer granularity can still reduce the occupancy to a reasonable level.

REFERENCES

[1] H. Braun, et al. CLIC 2008 parameters. CLIC-NOTE-764, 2008.

[2] S. Agostinelli et al. Geant4 – A Simulation Toolkit. Nucl. Instrum. Methods Phys. Res., Sect. A, vol. 506(3) pp. 250–303, 2003.

[3] P. Mora de Freitas and H. Videau. Detector Simulation with Mokka/Geant4 : Present and Future. In International Workshop on Linear Colliders (LCWS 2002). JeJu Island, Korea, 2002.
[4] A. Sailer. Update on forward region layout and backgrounds at CLIC. In Proceedings of the 18th FCal Collaboration Meeting. Predeal, Romania, 2011.
[5] D. Dannheim and A. Sailer. Beam-induced backgrounds in the CLIC detectors. LCD-Note-2011-021, 2011.

NEW RESULTS OF THE $\gamma\gamma$ BACKGROUND FOR LUMICAL IN CLIC

By

Rina SCHWARTZ[1]

(5) Tel Aviv University,Tel Aviv, Israel

The performance of the luminosity calorimeter for the CLIC detector is discussed in the absence and in the presence of background from incoherent-pair and $\gamma\gamma$ background from beamstrahlung. Implications for time stamping are presented.

Key words: Bhabha, CLIC, energy resolution, LumiCal, time stamping, incoherent-pairs, $\gamma\gamma$

1. INTRODUCTION

One of the main studies being done for the benefit of the luminosity measurement for the Compact Linear Collider (CLIC) is the analysis of beam-beam background flowing through the luminosity calorimeter (LumiCal). Bhabha scattering is the gauge process for the luminosity measurement, and LumiCal must be highly efficient to detect Bhabha events, so that the integrated luminosity is measured to a precision of 1% [1]. The measurement is based on energy and position reconstruction of the Bhabha-scattered electrons. First results on background from $\gamma\gamma$ reactions and their implications on the energy reconstruction are presented here, following the presentation given at the previous FCAL collaboration meeting in Predeal, Romania [2].

2. LUMICAL

Currently, LumiCal in CLIC is planned to have 40 layers in depth, each layer consisting of a silicon sensor plane, gap for electronics, and a tungsten absorber. The LumiCal geometrical volume ranges between polar angles $\theta = 37.7$ mrad and $\theta = 109.5$ mrad. It is centered around the outgoing beam axes, 2654.2 mm from the interaction point (IP). This is shown in Fig. 1, where LumiCal and BeamCal look slightly skewed compared to the rest of the sub-detectors which are centered on the incoming beams [3]. The inner radius of LumiCal is 100 mm, and the outer radius is 290 mm. In total, there are 64 × 48 × 40 pads in LumiCal (the numbers corresponds to radial, azimuthal and layer divisions of the silicon sensors, respectively) [3].

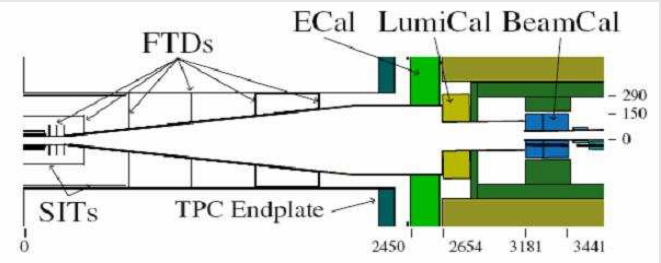

Figure 1. Forward Tracking and Calorimeters seen from the top.

3. TIME STRUCTURE AND BHABHA EVENTS RATE FOR LUMICAL IN CLIC

The time structure of the CLIC beams at center-of-mass energy of 3 TeV consists of bunch trains separated by 20 ns. There are 312 bunch crossings (BX) per train with 0.5 nsec separation, meaning 15,600 BX per second [4].

The physical Bhabha cross-section, which includes radiative effects, was obtained from the BHWIDE generator and is 101.016 pb. Assuming a luminosity of $5.9 \cdot 10^{34}$ $cm^{-2}s^{-1}$, a rate of 5.96 Hz is expected within the LumiCal geometrical volume, which approximately translates into one Bhabha scattering event every 10 trains.

More details regarding Bhabha events in LumiCal can be found in ref. [2].

4. BACKGROUND FROM $\gamma\gamma$ REACTIONS

Due to high bunch charge density in CLIC, each beam strongly radiates in presence of the other. This radiation may result in scattering of two photons into hadronic final states: $\gamma\gamma \rightarrow$ hadrons. The $\gamma\gamma \rightarrow$ hadrons events are distributed Poisson-like in time, with expectation value of 3.2 events per BX within the CLIC ILD detector acceptance at $\sqrt{s}$ = 3 TeV [5]. For the analysis presented here, a sample of 1600 events was used distributed into 473 BXs. The events were generated with GUINEA-PIG [7] and passed through the MOKKA [8] detector simulation.

The energy deposited in LumiCal by backround processes in one BX is subject to fluctuations. These fluctuations affect the energy resolution, and therefore must be studied carefully. An preliminary analysis of the $\gamma\gamma$ sample and the implications on the observed energy resolution of the LumiCal are presented.

It is useful to compare the $\gamma\gamma$ and incoherent-pairs backgrounds. For the incoherent-pairs analysis, a sample of 100 BX was used. More details about the latter analysis can be found in ref. [2], here only the relevant results will be presented here.

4.1 Characteristics of $\gamma\gamma$ events

The generated background particles are mostly photons and pions (approx. 46% and 40%, respectively); amongst them, 45% are generated at polar angles within 110 mrad around the beam line, and their energy ranges between 10 MeV and 100 GeV, as shown in Fig. 2.

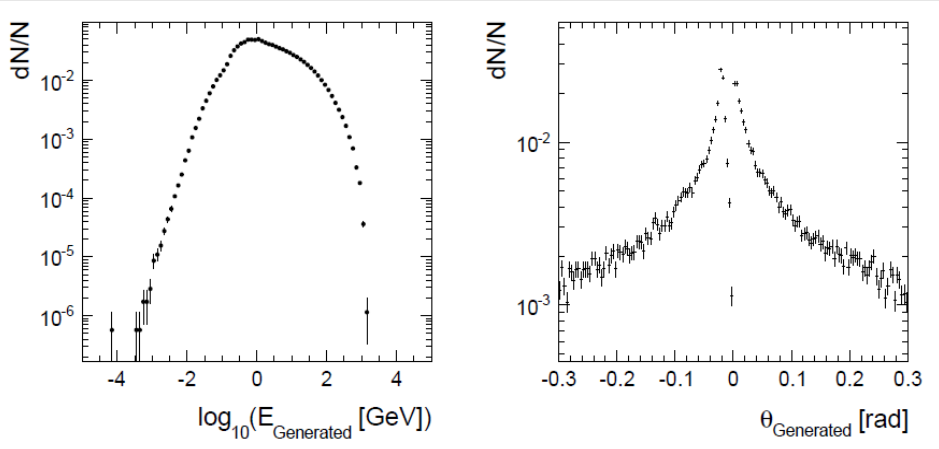

Figure 2. Distributions of energy (left) and of polar angle (right) of particles originating from $\gamma\gamma$ background.

4.2 Background in LumiCal

The relative contributions of Bhabha electrons signal and both background sources can be seen in Fig. 3, where the longitudinal charge deposit profile of an electron is overlayed with the expected accumulated background deposits from 20 BX (benchmark for readout sampling rate [6]). The background is not uniformly distributed over the volume of LumiCal. In the maximum of the shower, the background may contribute up to about 1% of the energy. In the last layers the background is nearly comparable to the signal. On average, the total charge deposited by a single electron is about 785 pC, whereas the total charge accumulated in LumiCal due to 20 BX of background is ~8 pC from $\gamma\gamma$, and ~3 pC from incoherent pairs.

The distributions of background charge deposits in a single pad are shown in Fig. 4, and are within currently known ADC limits [6]. Depicted in Fig. 5 is the occupancy per BX of incoherent pairs and of $\gamma\gamma$ background events. Keeping in mind the limited readout resolution, only pads with signal higher than 0.2 MIP were counted. The occupancy is not uniformly distributed over the volume of LumiCal. For incoherent pairs it is highest around the inner-most rings of LumiCal, and in the back layers. For $\gamma\gamma$, the highest occupancy is in the front layers and low radii.

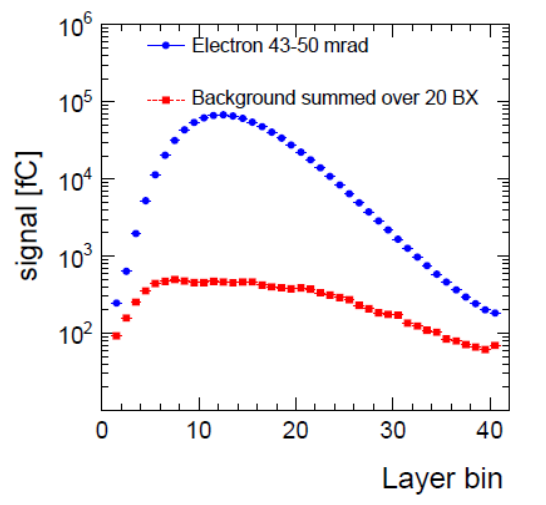

Figure 3. Charge deposit profile of the e^- signal (blue dots) as a function of the layer number in LumiCal, overlayed with background signal in e^- pads (red squares), summed over 20 BX.

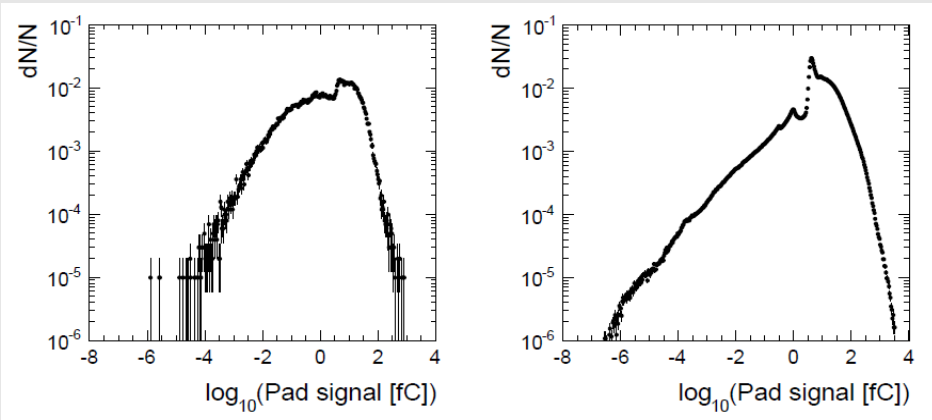

Figure 4. Left: distribution of charge depositions in a single pad from incoherent pairs. Right: same for $\gamma\gamma$.

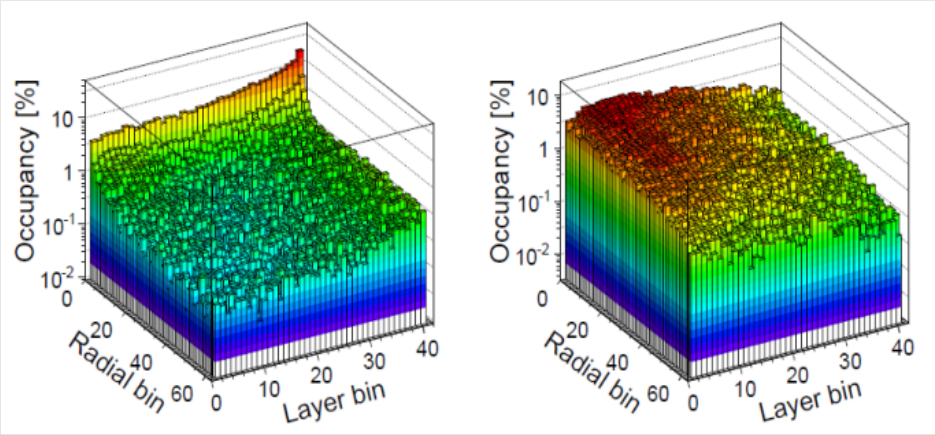

Figure 5. Left: the occupancy of energy deposition in LumiCal pads from incoherent pairs, with 0.2 MIP cut. Right: same for $\gamma\gamma$.

5. EFFECT ON ENERGY RESOLUTION

The energy resolution coefficient, a_{res}, is defined as following:

$$\frac{a_{res}}{\sqrt{E_b(\mathrm{GeV})}} = \frac{\sigma_e}{E_m} \qquad (1)$$

where E_b is the beam energy, σ_e and E_m are given in GeV, and are the standard deviation and the mean of the deposited energy distribution (which is Gaussian [1]), respectively. The contribution of the background to the resolution will depend on the time stamping. Assuming integration over BXs, the energy resolution coefficient with background, a_{res}^{wb}, is defined as following:

$$\frac{a_{res}^{wb}}{\sqrt{E_b(\mathrm{GeV})}} = \frac{\sqrt{\sigma_e^2 + N_{BX}\sigma_{bgr}^2}}{E_m} \qquad (2)$$

where N_{BX} is the number of integrated BXs and σ_{bgr} is the RMS of the background energy deposits in the e^- pads. The resolution without and with background is shown in Fig. 6 as a function of the impact angle, for different values of N_{BX}. As expected, accumulation of background energy depositions over many BX adds fluctuations and hence deteriorates the energy resolution. Without background, the resolution deteriorates below 43 mrad due to leakage and above 80 mrad due to the detector geometry (presumably the overlap between ECal and LumiCal). The contribution of the $\gamma\gamma$ (incoherent pairs) background in this fiducial volume, if summed over a full train, may deteriorate the resolution by as much as 90% (10%). Summing over 20 BX may deteriorate the resolution by up to than 10% (1%). A study is currently being conducted to increase the statistics and combine results from both background classes.

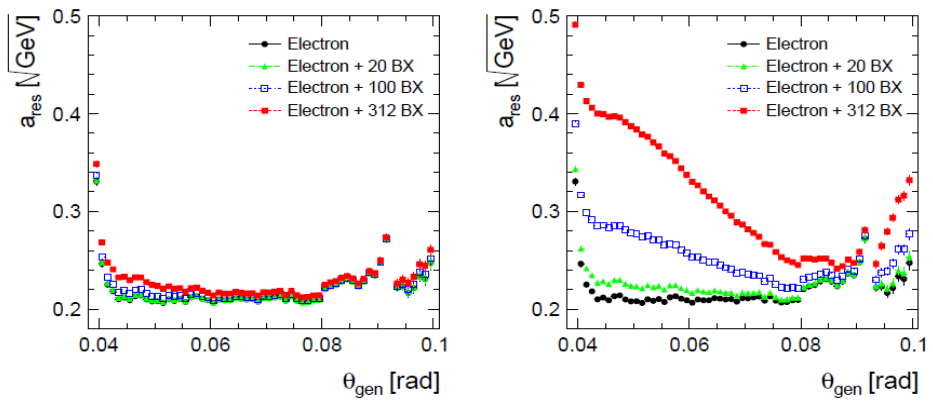

Figure 6. Measure of the energy resolution, a_{res}, as a function of the e^- polar angle, θ_{gen}, without and with background, integrated over different number of BXs, as depicted in the figure. The left (right) plot presents results of incoherent pairs ($\gamma\gamma$) background.

6. SUMMARY

An overview of $\gamma\gamma$ background for LumiCal in CLIC was presented. The background charge deposits distribution in LumiCal was studied. The fiducial volume is defined by the nominal LumiCal energy resolution ($a_{res} = 0.21$) to be $43 < \theta < 80$ mrad. In this angular range, the $\gamma\gamma$ background fluctuations of 20 BX deteriorate the energy resolution by up to 10%. Next, the results presented here will be reproduced with a larger sample of BX, and implications for time stamping will be further explored.

ACKNOWLEDGMENTS

This research was partially funded by the Israel Science Foundation.

REFERENCES

[1] H. Abramowicz et al., A luminosity calorimeter for CLIC, Technical Report LCD-Note-2009-02, CERN LCD, 2009.

[2] R. Schwartz, LumiCal performance in the CLIC environment - Progress report, Proceedings of the 18th FCAL Collaboration Workshop, Predeal, Romania, 2011.

[3] A. Munnich, A. Sailer, The CLIC-ILD-CDR geometry for the CDR Monte-Carlo mass production, LCD-2011-002, 2011.

[4] L. Linssen, Physics and detector studies for the CLIC multi-TeV e+e- collider, CERN report 2004-5, 2009.

[5] CLIC CDR (under review): http://project-clic-cdr.web.cern.ch/project-CLIC-CDR/CDR_Volume1.pdf

[6] S. Kulis, M. Idzik, Study of readout architectures for trigerless high event rate detectors at CLIC, Technical Report LCD-Note-2011-015, CERN LCD, 2011.

[7] D. Schulte., GUINEA-PIG: http://www-sldnt.slac.stanford.edu/snowmass/Software/GuineaPig

[8] Detector simulation MOKKA7: http://polzope.in2p3.fr:8081/MOKKA7

BACKGROUNDS AT CLIC

By

Ivan SMILJANIĆ[1], Mila PANDUROVIĆ[1], Strahinja LUKIĆ[1] AND Ivanka BOŽOVIĆ JELISAVČIĆ[1]

(1) Vinča Institute of Nuclear Sciences, Belgrade, Serbia

In this paper we discuss characteristics of physics and beam-induced backgrounds in luminosity calorimeter at the future Compact Linear Collider (CLIC) operating at the cms energy of 3 TeV. Presence of several sources of background is taken into account: SM four-fermion production, hadronic background and incoherent pairs converted from beamstrahlung photons. It has been concluded that by proper selection the presence of backgrounds in the luminosity calorimeter can be maintained at the upper limit of 10^{-3} w.r.t. signal. However, the main issue will be to define a region of the luminosity spectrum where the integral luminosity will be measured, since the luminosity spectrum is very strongly influenced by the beam-beam interaction related effects.

Key words: luminosity measurement background, CLIC, BHSE

INTRODUCTION

In this study, several processes are considered as a potential background in luminosity calorimeter (LumiCal), version CLIC_ILD [1], at (CLIC. The main source of background comes from the four-fermion production via NC mechanism while the presence of hadrons or incoherent pairs produced through conversion or interaction of beamstrahlung photons with another electron or a photon is also quantified as a potential miscount.

Due to the relatively large cross-section, and possibility to accurately calculate the cross-section from theory, small-angle Bhabha scattering is used to measure and monitor the luminosity in electron-positron colliders, such as the International Linear Collider (ILC). Measurement of the event rate of the Bhabha scattering process in the luminosity calorimeter at very small polar angles in the very forward region is a way to determine luminosity at the ILC [2]. However, since the effective suppression of the Bhabha cross-section (BHSE) in the luminometer fiducial volume at CLIC is over 70% primarily due to loss of the available center-of-mass energy on beamstrahlung, the main idea is to define a region in the vicinity of the nominal cms energy where systematic effects, primarily BHSE, can be controlled with satisfying accuracy of 10^{-2} or better.

Here we will demonstrate that, in principle, it is possible to introduce a selection that will lead to an overall background suppression at the required level.

Luminosity calorimeter at CLIC has been designed for the precise determination of the total luminosity. In CLIC_ILD geometry, LumiCal consists of 40 longitudinal layers of silicon sensors segmented in pads with 64 radial and 48 azimuthal segments in each layer, which ensure an efficient selection of Bhabha events [3] and a precise shower position measurement. Sensor layers are followed by the tungsten absorber and the interconnection structure. LumiCal covers polar angles between

37.7 mrad and 109.5 mrad [4]. It is located at about 2.6 m from the IP, right behind the ECAL, with the edge of the ECAL shadowing the outer perimeter of the LumiCal (see Figure 1) [1].

The requirement of shower containment for the Bhabha scattering final states and the scattering off the ECAL edge limit the fiducial volume of the LumiCal at CLIC_ILD to the range 43 mrad to 80 mrad [5].

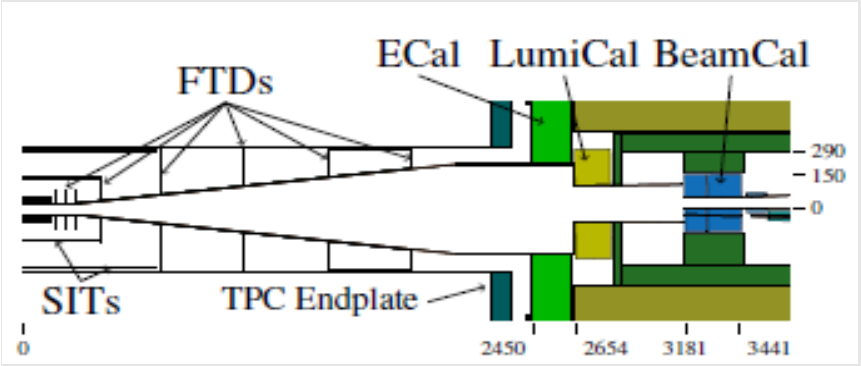

Figure 1. The very forward region of the CLIC detector.

METHOD

In principle, integrated luminosity can be determined from the total number of Bhabha events, N_{th}, produced in the acceptance region of the luminosity calorimeter and the corresponding theoretical cross-section σ_B.

$$L_{\text{int}} = \frac{N_{th}}{\sigma_B} \qquad (1)$$

The number of counted Bhabha events, N_{exp}, has to be corrected for the number of background events misidentified as Bhabhas, N_{bck}, and for the selection efficiency ε. Also, if known, other corrections can be introduced. Uncertainty of the corrections will result in systematic uncertainty of the measured luminosity.

$$L_{\text{int}} = \frac{N_{\text{exp}} - N_{bck}}{\varepsilon \cdot \sigma_B} \qquad (2)$$

Bhabha events (10 000) are generated using BHWIDE 1.04 generator [6], within the fiducial volume of LumiCal (43 mrad < θ < 80 mrad). Corresponding cross-section is σ_{bha}=45.9±0.4 pb. Leptonic and hadronic four-fermion background (100 000 events each) is generated using WHIZARD 1.40 [7] in the angular range $0.05^o < \theta < 179.95^o$, with the transferred momentum of 10 MeV. Corresponding cross-sections are σ_{lep}=73.7±0.4 pb and σ_{had}=22.7±0.2 pb.

Background induced by beamstrahlung photons is generated using GuineaPig 1.2 [8]. 100 bunch crossings is simulated to produce incoherent pairs (100 bunch crossings) and 1 million bunch crossings corresponding to $\gamma\gamma \rightarrow hadron$ conversion.

RESULTS

Figure 2a and 2b show distributions of energy and polar angle of leptons from physics background in the full angular range respectively. Figures 3a and 3b show the same distributions in the fiducial volume of LumiCal. If we define a spectator as an electron carrying more than 60% of the beam energy, it can be seen that 23.5% of all the particles are such a high-energy electrons and that 0.8% of spectators enter LumiCal since the most of spectators are emitted close to the beam pipe at smaller polar angles. Similarly, in the case of hadronic physics background, 8% of all particles are spectators, and 0.5% of spectators enter the fiducial volume of

LumiCal [9].

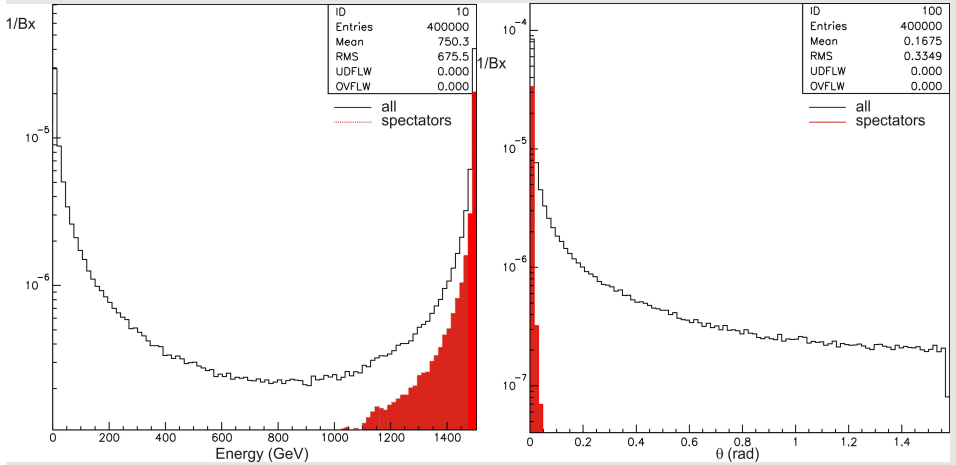

(a) (b)

Figure 2. (a) Energy and (b) θ distribution of leptons from physics background in the full angular range.

Beamstrahlung photons interacting with other electrons or photons may produce incoherent e^+e^- pairs (~10^5 per BX), while by far the most dominant beam-induced process originates from the direct beamstrahlung photon conversion in a strong microscopic EM field [10]. However, coherent pairs are emitted far below the LumiCal. A sample containing 100 bunch crossings (~30 M particles) of incoherent pairs has been studied. In the first instance, particles that enter the fiducial volume of LumiCal are investigated. Results are shown at Figures 4a and 4b. As can be seen in Figure 4b, none of particles in the fiducial volume of LumiCal will carry energy above 80 GeV within 100 bunch crossings.

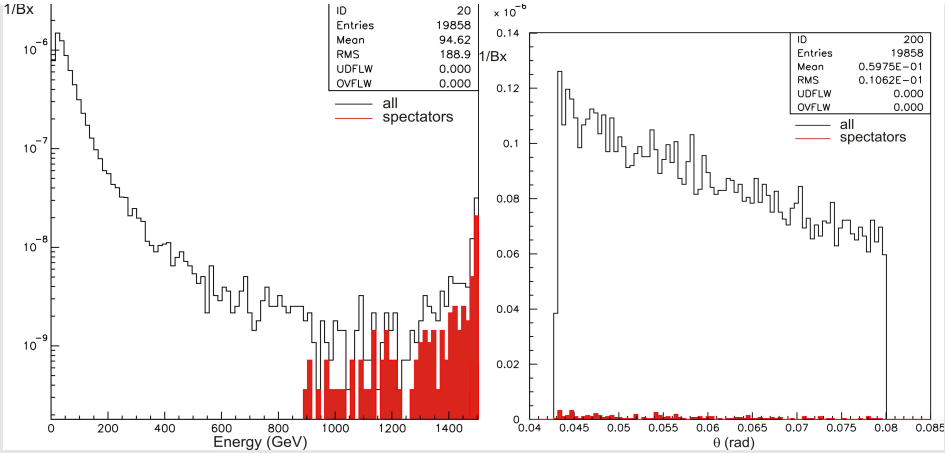

(a) (b)

Figure 3. (a) Energy and (b) θ distribution of leptons from physics background in the fiducial volume of LumiCal.

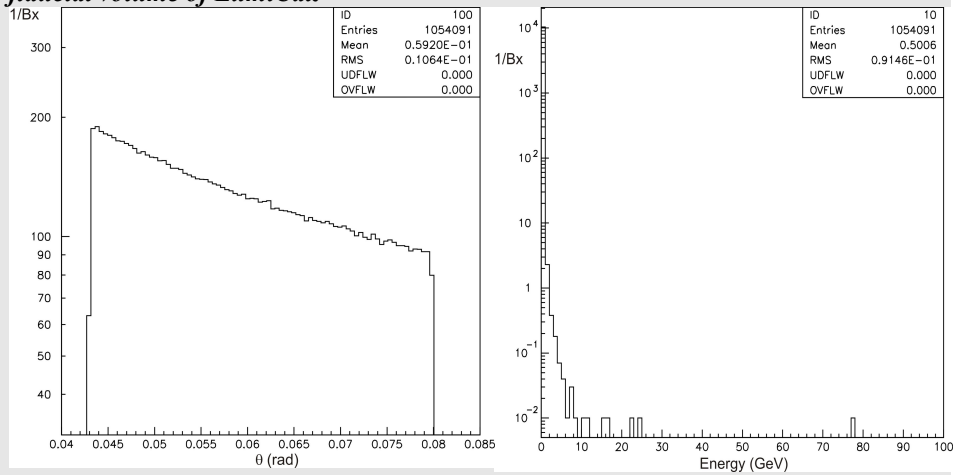

(a) (b)

Figure 4. (a) θ and (b) Energy distribution of incoherent pairs in the fiducial volume of LumiCal.

Secondly, polar angle distribution of particles carrying the energy above 60% of the beam energy (900 MeV) is investigated. Result is shown at Figure 5. Apparently, none of the investigated particles enter the fiducial volume of LumiCal. In order to establish the upper limit for B/S of 10^{-3} for incoherent pairs, $2.6 \cdot 10^{6}$ bunch crossings is needed.

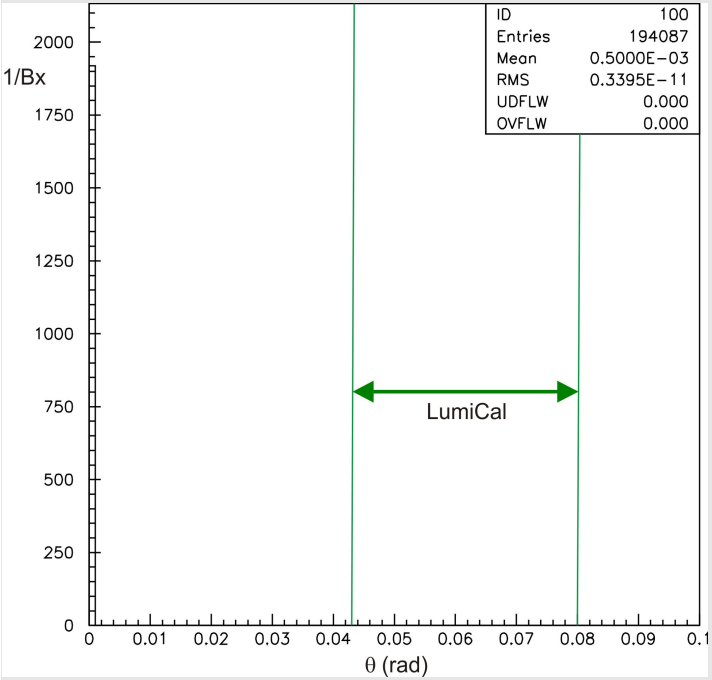

Figure 5. θ distribution of incoherent pairs carrying the energy above 60% of the beam energy

$\gamma\gamma \rightarrow hadron$ is the interaction of real beamstrahlung photons (3.2 per BX [10]) into quark pairs. There is also some contribution due to virtual photons from beam particles. 1 million bunch crossings (~7.2 million events) of this type is generated using GuineaPig 1.2. Energy distribution of these photons is shown on Figure 6a Only for the purpose to estimate available energy of the hadronizaton products the obtained initial state distribution of $\gamma\gamma$ pairs is then treated as the $e^{+}e^{-}$ distribution, e.g. $\gamma\gamma$ pairs are treated as $e^{+}e^{-}$ pairs. As can be seen from Figure 6b, only a few pairs of beamstrahlung photons in 10 000 bunch crossings will carry more than 0.8 cms energy.

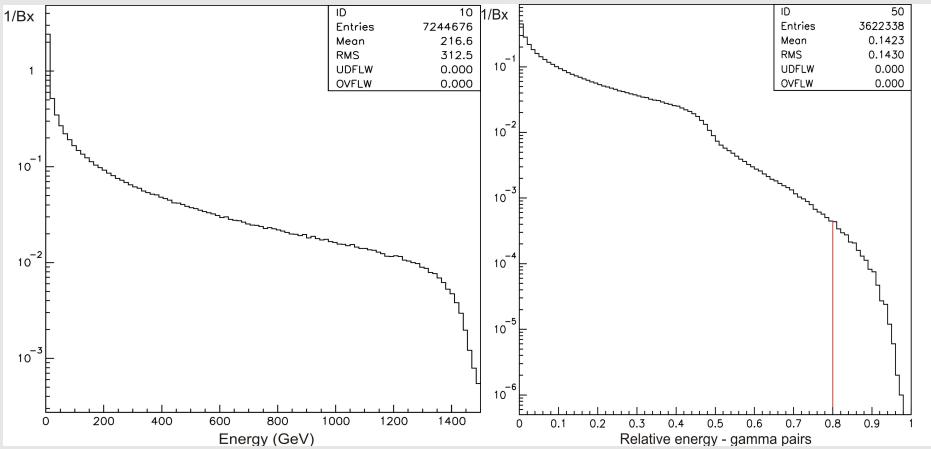

(a) (b)

Figure 6. Energy distribution of photons generated using GuineaPig; (b) Distribution of energy of beamstrahlung pairs normalized to the nominal cms energy.

According to these results, the upper limit of B/S ratio originating from this effect is 6.4.

POSSIBLE SELECTION CRITERIA

Selection criteria used in this study are basically derived from a similar study performed at ILC [11] and they are set as follows:

- asymmetric cuts on θ - these cuts are applied subsequently to forward and backward sides of the detector. Therefore, cuts are set as follows: cut 1: 47 < θ < 73 mrad; cut 2: 43 < θ < 80 mrad. These cuts are taken only as illustration of the background suppression power of the cuts optimized for ILC, making no particular sense for BHSE reduction in the CLIC case [12];
- cut on relative energy,

$$E_{rel} = \frac{E_i + E_j}{2 \cdot E_{beam}}, E_{rel} > 0.8; \quad (3)$$

Figure 1. cut on acoplanarity, Δφ (difference in φ between two particles belonging to a pair that enters the LumiCal); we took Δφ <174.5 mrad (10°);

Figure 2. cuts on acolinearity, Δθ (difference in θ between two particles belonging to a pair that enters the LumiCal): Δθ <1.75 mrad (0.1°) and Δθ<8.73 mrad (0.5°);

Ratio of physics background to signal using different combination of these cuts is shown in Table 1.

Table 1. Physics background at CLIC

	Asym. cuts+ E_{rel}	**E_{rel} + Δφ**	**Asym. cuts + E_{rel} + Δφ**	**E_{rel} + Δφ + Δθ<0.1°**	**E_{rel} + Δφ + Δθ<0.5°**
B_{lept}/S (x10^{-4})	8.07	5.03	5.74	2.05	4.13
Δ(B_{lept}/S) (%)	±19	±20	±22.5	±34.5	±30
B_{hadr}/S (x10^{-4})	1.76	1.03	1.21	0.28	0.73
Δ(B_{hadr}/S) (%)	±22.5	±25	±27	±51	±30
B_{tot}/S (x10^{-4})	9.85	6.06	6.95	2.33	4.86
Δ(B_{tot}/S) (%)	±16	±17	±19	±31	±20
Cut efficiency (%)	66.4	92.9	66.3	75.8	88.0

CONCLUSION

Once the region of interest to measure integral luminosity is determined on luminosity spectrum, various event selectons can be used in order to suppress either physics or beam-induced background.

It has been demonstrated that physics background at CLIC can be in principle controlled at the level of 10^{-3} or better.

A huge statistics (~10^7 bunch crossings) of incoherent pairs is needed to set the B/S component from incoherent pairs to ≤10^{-3}. GuineaPig has to be upgraded to allow this.

REFERENCES

[1] A.Műnnich and A. Sailer, The CLIC ILD CDR Geometry for the CDR Monte Carlo Mass Production. LCD-Note-2011-002, 2011.

[2] International Linear Collider; Reference Design Report, April 2007, http://www.linearcollider.org/cms/

[3] I. Bozovic-Jelisavcic et al., Luminosity measurement at ILC, (2010), arXiv:1006.2539

[4] CLIC conceptual design report Vol. 2: Physics and detectors at CLIC

[5] R. Schwartz, LumiCal performance in the CLIC environment, Proceedings of the 18th FCAL Collaboration Workshop, ISBN: 978-973-0-11117-0

[6] S. Jadach, W. Placzek and B.F.L. Ward, BHWIDE 1.00: O(α) YFS Exponentiated Monte Carlo for Bhabha Scattering at Wide Angles for LEP1/SLC and LEP2, Phys. Lett. B390 (1997) 298.

[7] W. Kilian, T. Ohl, J. Reuter, WHIZARD: Simulating Multi-Particle Processes at LHC and ILC, arXiv: 0708.4233 [hep-ph]

[8] D. Schulte, Beam-Beam Simulations with GUINEA-PIG. In 5th International Computational Accelerator Physics Conference. Monterey, CA, USA, 1998. CLIC-NOTE 387.

[9] I. Smiljanić, Physics background at CLIC, presentation given at the 19th FCAL Workshop, Belgrade, http://www.vinca.rs/hep/pub/Ivan_FCAL_Bgd.pdf

[10] A.Sailer, Update on forward region Layout and background at CLIC, Proceedings of the 18th FCAL Collaboration Workshop, ISBN: 978-973-0-11117-0

[11] M. Pandurović, I. Božović Jelisavčić, Physics background in luminosity measurement at 1TEV at ILC, Proceedings of the XIX Workshop on Forward Calorimetry at Future Linear Collider

[12] S. Lukić, The Bhabha Suppression Effect revisited, Proceedings of the XIX Workshop on Forward Calorimetry at Future Linear Collider